Christopher Lamprecht, BSc

Realisation of an Optical Ethernet Transceiver Modem for 1550nm Earth-Space FSO Transmission

Master's Thesis
to achieve the university degree of
Master of Science
Master's degree programme: Information and Computer Engineering

submitted to

Graz University of Technology

Supervisor
Ao.Univ.-Prof. Dipl.-Ing. Dr.techn. Erich Leitgeb

Institute of Microwave and Photonic Engineering
Head: Univ.-Prof. Dipl.-Ing. Dr.techn. MBA Wolgang Bösch

Graz, August 2020

Affidavit

I declare that I have authored this thesis independently, that I have not used other than the declared sources/resources, and that I have explicitly indicated all material which has been quoted either literally or by content from the sources used. The text document uploaded to TUGRAZonline is identical to the present master's thesis.

_____   _____
          Date   Signature

Acknowledgements

First of all, i would like to thank my supervisor and mentor Erich Leitgeb who supported me throughout my whole master's programme and offered me this master's thesis. To every problem which came up during my studies, he offered a solution and encouraged me with my thesis.

Special thanks goes to ASA Astrosysteme GmbH and Egon Döberl who made this thesis possible and gave us financial support. I am looking forward to working with you on future projects.

I would also like to thank Pirmin Pezzei, who always had an open ear for my problems which arose throughout this thesis and also for supporting me with the measurements in the laboratory.

Also, a big thank you to my colleagues in the optical laboratory, who always offered me their help and support in the design and measurement phase.

A big thank you also goes to the whole Institute of Microwave and Photonic Engineering. Various colleagues showed their support and help.

Last but not least, i would like to thank my family for the continuous support throughout my life's journey. Without them, none of this would have been possible.

Abstract

Free space optical communication gained popularity in the recent years, due to the high data rates optical communication systems are feasible. Research has increased, particularly in aerospace applications where large amounts of data are transmitted over long distances. Various new missions are planned by aerospace organizations such as ESA or NASA, which provide an optical communication link in addition to the high-frequency link that is typically used. Especially in deep space communications, optical links gained interest due to the lack of atmospheric effects in space. Hence, the major disadvantage for optical communication systems, namely attenuation due to atmospheric effects, is absent. Also, compared to regular high frequency links, much higher data rates can be achieved with optical communication systems. However, the optical data needs to be translated back into the electrical domain, in order to process the data collected by satellites, probes or other spacecrafts.

This thesis gives an overview of optical communication and proposes a bidirectional modem which translates optical signals into electrical Ethernet frames and vice versa. The idea is to translate all optical signals into electrical signals, regardless of the used protocol. The optical signals are translated into the electrical domain using bidirectional small form-factor pluggable (SFP) modules. In combination with media converters, Ethernet frames are generated which can be further distributed throughout the local area network. The master's thesis was done in cooperation with ASA Astrosysteme GmbH.

Kurzfassung

Optische Kommunikationssysteme wurden, aufgrund der hohen Datenraten, in den letzten Jahren immer beliebter. Insbesondere in Luft- und Raumfahrtsystemen, in denen große Datenmengen über große Entfernungen übertragen werden, hat die Forschung zugenommen. Luft- und Raumfahrtorganisationen wie ESA und NASA planen diverse neue Missionen, welche zusätzlich zum üblicherweise verwendeten Hochfrequenzübertragungskanal eine optische Kommunikationsverbindung bereitstellen. Einer der großen Nachteile für optische Kommunikationssysteme, nämlich die Dämpfung des Signals aufgrund atmosphärischer Effekte, ist im Weltraum nicht vorhanden. Aus diesem Grund verstärkte sich das Interesse, speziell in der Deep Space Weltraumkommunikation, an opischen Kommunikationessystemen. Im Vergleich zu regulären Hochfrequenzverbindungen können mit optischen Kommunikationssystemen viel höhere Datenraten erzielt werden. Die optischen Daten müssen jedoch irgendwann zurück in die elektrischen Domäne übersetzt werden, damit die von Satelliten, Sonden oder anderen Raumfahrzeugen gesammelten Daten verarbeitet werden können.

Diese Arbeit befasst sich mit der Aufarbeitung optischer Kommunikationssysteme und stellt ein bidirektionales Modem vor, welches optische Signale in elektrische Ethernet-Frames übersetzt und vice versa. Die Idee dahinter ist, alle optischen Signale unabhängig vom verwendeten (proprietären) Protokoll in elektrische Signale umzuwandeln. Die optischen Signale werden unter Verwendung von bidirektionalen SFP-Modulen (Small Form Factor Pluggable) in den elektrischen Bereich übersetzt. In Kombination mit Medienkonvertern werden Ethernet-Frames generiert, die im gesamten lokalen Netzwerk weiter verteilt werden können. Die Masterarbeit wurde in Zusammenarbeit mit der ASA Astrosysteme GmbH erstellt.

Contents

List of Figures

1 Introduction

NASA extended its optical communications program and is planning to integrate laser communication into the existing operational space network by 2025 [1], due to the prior success of the Lunar Laser Communications Demonstration (LLCD) [2]. High data rates are feasible for optical communication systems, which is particularly advantageous for satellite communication. The german aerospace center demonstrated a free space optical (FSO) data transmission using data rates of 13.16 Tbps [3]. Such high data rates cannot be achieved by regular radio frequency (RF) communication systems to this date, which is why optical communication got more attention by researchers and the aerospace industry in the recent years.

The narrow beam width and the usage of the latest optical detector technologies allow data transmission over high ranges, making FSO systems even suitable for deep space missions. NASAs Psyche mission spacecraft is equipped with a flight laser transceiver (FLT) which was especially developed for deep space optical communications (DSOC) [4]. The FLT operates at 1550nm wavelength and 4W optical power which allows a link distance of up to 2AU or 299.2 million kilometres to the Psyche asteroid. The Psyche mission launch is planned in August 2022 and the spacecraft will arrive at the asteroid Psyche at the end of January 2026 [5].

Optical communication is not only relevant in deep space mission, but also in low earth orbit (LEO) and geostationary orbit (GEO) constellations. A successful optical link between the Artemis GEO satellite and the SPOT-4 LEO satellite has been established in 2001 within the SILEX (Semiconductor Inter-satellite Link Experiment) project [6][7]. Besides transmitting earth observation data, collected by the SPOT-4 earth observation satellite, also bit error rate measurements were subject to the SILEX project. Also inter-satellite link acquisition, optical ground station acquisition and tracking experiments have been performed. The SILEX project achieved excellent results in its experiments, which caused further research in optical satellite communication links.

Space-to-earth communication is especially important, since all the data collected in space needs to be further processed on earth. While in deep space the optical signal only suffers from the free space loss, in space-to-earth communication the signal is also affected by atmospheric effects like precipitation, fog or atmospheric turbulences. These atmospheric effects induce attenuation, due to particle absorption or scattering, especially *Mie* scattering. Beam wandering and scintillation effects occur, due to atmospheric turbulences and the resulting fluctuations of the refractive index profile of the atmosphere. These losses need to be considered in the design of the FSO system.

Due to the atmospheric effects on optical signals, also RF-Optical hybrid solutions have been proposed [8]. Under clear sky conditions the optical link can be used to transmit the data on high data rates, whereas in fog or precipitation scenarios the data is transmitted over the RF link in order to mitigate the high losses in the optical domain, due to fog or clouds. Hence, the link availability is kept high due to the hybrid solution and also high data rates can be achieved under clear sky or slightly cloudy conditions, which overall extends the capabilities of plain RF satellite communications. The received optical satellite signal, needs to be translated back into electrical signals in order for computers to process and distributed the collected data. This thesis proposes a modem which translates optical signals into the Ethernet domain and vice versa in order to process the optical signals, received from satellites. Together with *ASA Astrosysteme GmbH* an optical transceiver modem was developed which translates an optical satellite signal, into electrical Ethernet frames and vice versa. The Ethernet frames can then be further distributed over the local area network (LAN). The optical satellite signal is captured by a telescope, developed by *ASA Astrosysteme GmbH*. The optical satellite tracking is done by *Vienna University of Technology (TU Wien)*. The translation of the optical signals into electrical Ethernet frames is the objective of this thesis.

Outline

At the beginning a short introduction into optical communication will be given, which explains where and why we use optical communication. The introduction is followed by the theoretical background in optical communication which covers free space optical communication, atmospheric effects, fibres and optical modulation schemes. The chapter to free space optical communication gives at first a short introduction, followed by why we use certain wavelengths in FSO communication systems and an explanation to the link budget calculation, which is crucial for an FSO system design. Fog, clouds, precipitation events, atmospheric turbulences are covered in the chapter to atmospheric effects which will give an overview about the challenges we have to face, when designing an FSO system which operates on earth. FSO systems also use optical fibres to transmit data within the system, for this reason also optical fibres are covered in this thesis. The chapter to optical fibres covers the overall physical structure of an optical fibre cable, the principle of total reflection and why optical fibres actually work, and finally a brief description of single mode and multi mode fibres. The two main modulation schemes, on-off-keying and pulse position modulation, are covered in the chapter to modulation schemes. After the theory to optical communication, the system design of the optical Ethernet transceiver modem will be described which is the main objective of this thesis. First the overall system is described, followed by the individual parts which are used for the optical transceiver modem. After the system design the measurements are described and evaluated. Three measurements are performed in order to evaluate the capabilities of the optical Ethernet transceiver modem. First the bit rate on the Ethernet-to-Ethernet link is measured and analysed using a, especially for this purpose developed, software. The second measurement evaluates the Ethernet-to-optical link and shows that the data, received at the Ethernet interface, is translated into the corresponding optical signals. The last measurement setup translates received optical signals into Ethernet frames, which can then be further distributed over the local area network. This measurement is especially important, since the main purpose of this module is to translate optical signals, received from satellites, into electrical Ethernet frames, in order to analyse and post-process the data collected by the satellite. The thesis ends with a conclusion of the system and the overall measurement results.

2 Theory

In this chapter, a theoretical overview in optical communication is given. The focus will be in free space optical (FSO) communication and atmospheric effects. Since optical fibres also play a major role in such systems and especially in this thesis, a description on optical fibres will also be given. Also the most common modulation schemes in optical communication systems are described.

2.1 Free space optical communication

The obvious advantage of free space optical (FSO) communication is, that the data is directly transmitted over air or free space and no cables are needed. Especially for last-mile connectivity, FSO systems deliver a cost effective broadband solution, which makes this very suitable for inner city telecommunication services [9]. FSO communication is not only suitable for terrestrial applications, but also for aerospace or extraterrestrial applications. Earth observation satellites in low earth orbit (LEO) usually capture a lot of data in a small period of time. Large amounts of data need to be transferred down to earth in a timely manner, due to the low visibility time windows of 10 minutes in LEO. FSO systems are well known for their ability to transmit at high data rates, making these systems very interesting for aerospace applications and deep space missions.

2.1.1 Choice of wavelength

Since different wavelengths undergo different attenuation and dispersion effects, it is crucial to select the right wavelength. Due to the transmission properties of optical fibres, three transmission windows have been established in the past years. The first optical transmission window is at 850nm. In the early days of optical communications, LEDs mostly operated at

this wavelength. Therefore the 850nm define the first transmission window. Later on lasers were used for optical communication. There wavelengths of 1300nm (second transmission window) and 1550nm (third transmission window) have been established, due to the low material absorption and therefore low attenuation at these wavelengths in fibres (see figure 2.1).

Also dispersion effects are spectrally dependent in optical fibres. In figure 2.2 it can be seen that the dispersion is 0ps/(nm km) at a wavelength $\lambda_0 = 1310nm$. At this wavelength, no material dispersion occurs, which makes the second transmission window also very suitable for optical fibre communication.

Since the three transmission windows are so well established, they are also used in free space optical communication. In some literature a wavelength of 1550nm is preferred, due to the lower attenuation at this wavelength. However, this is a common misconception, since in free space optical communication, the difference in attenuation between i.e. 785nm and 1550nm is rather small for clear sky conditions and negligibly small in fog conditions [11]. The choice of the wavelength at 1550nm still makes sense, due to eye safety reasons [12]. Laser light with a wavelength greater than 1400nm is mostly absorbed by the cornea. Wavelengths smaller than 1400nm can reach the retina, which may lead to severe damage of the retina. Also the eye lens is focusing the laser beam on a small spot, which increases the damage to the retina. A wavelength of 1550nm is well suited, since it does not lead to a severe retinal damage compared to smaller wavelengths. Therefore higher optical powers for free space optical transmission can be used, while eye safety is still provided. According to the American National Standards Institute (ANSI) the maximum power for a 10 second exposure to laser light is at $1mW/cm^2$ for wavelengths of $\lambda = 800nm$ and $100mW/cm^2$ for wavelengths of $\lambda = 1550nm$. Hence, if a wavelength of $\lambda = 1550nm$ is used, the optical output power of the laser can be a hundred times higher as if a wavelength of $\lambda = 800nm$ is used, while still providing eye safety.
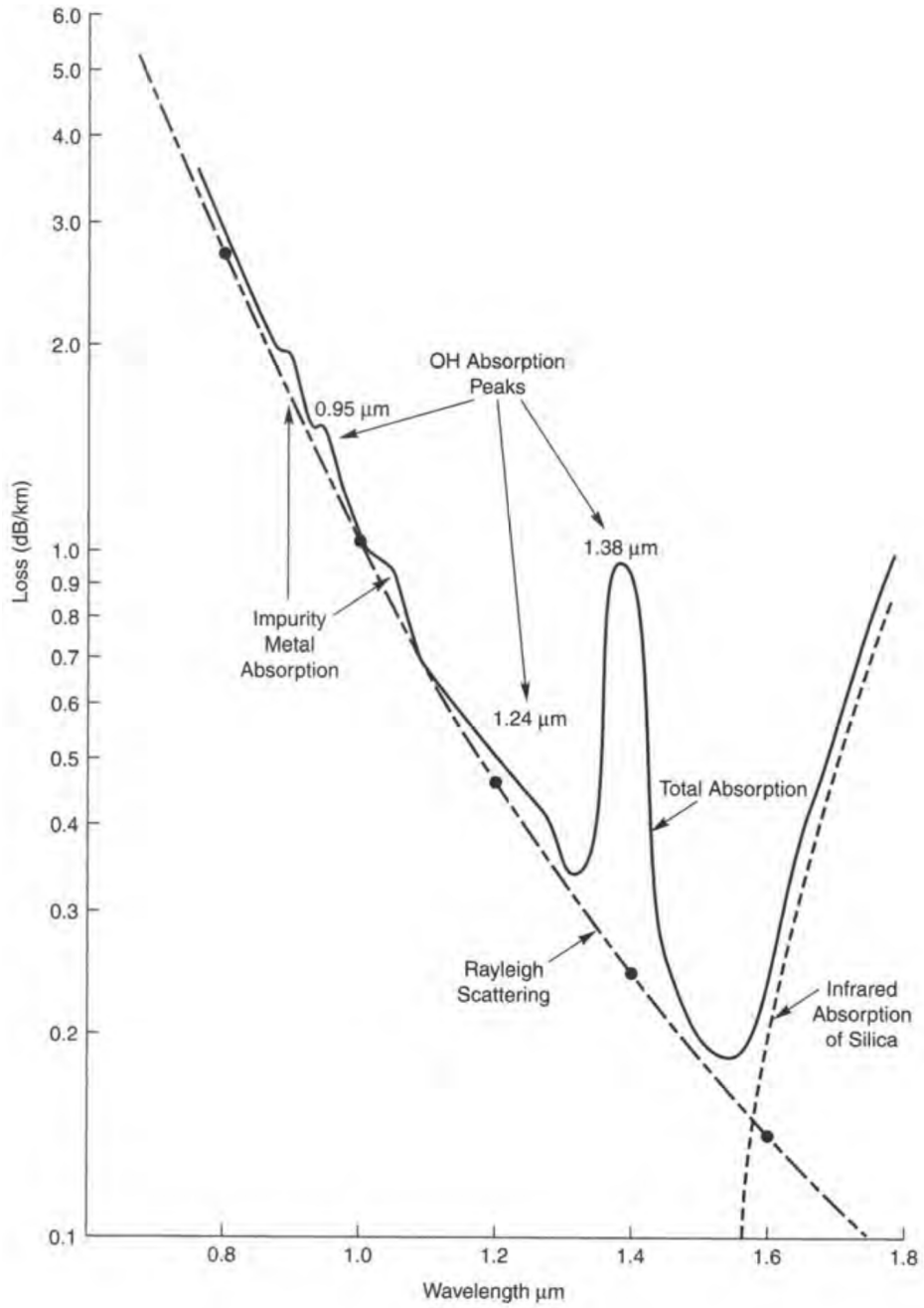
Figure 2.1: Optical attenuation with respect to the wavelength λ [10]
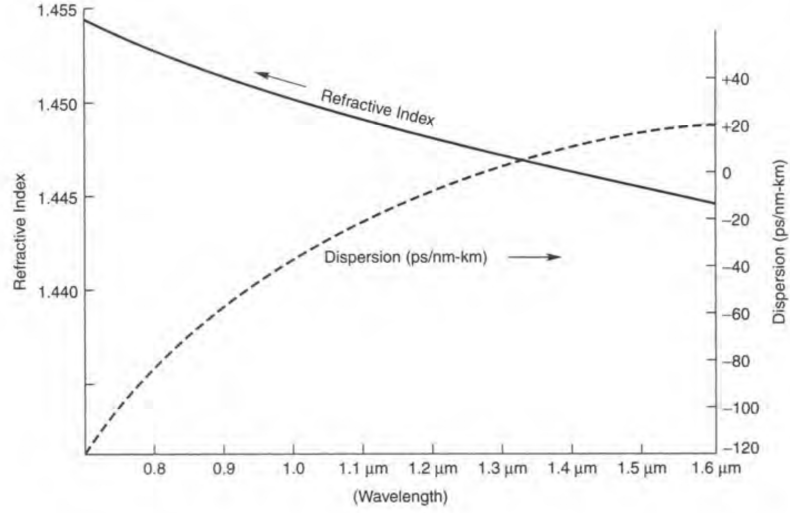
Figure 2.2: Dispersion effects for optical fibre communication [10]

2.1.2 Link budget

To design a FSO system, it is necessary to compute the link budget in order to estimate the performance of the system. This can be done using the range equation to calculate the received power P_R described in *Free-Space Laser Communications* [13] as follows:

$$P_R = P_T G_T \tau_T \tau_{ATM} L_{FS} G_R \tau_R \tag{2.1}$$

Where P_T is the optical output output power of the transmitter. G_T and G_R is the gain of the transmitter and the receiver respectively. τ_T and τ_R are the optical efficiencies of the transmitter and the receiver respectively. The value of the atmospheric transmission is given by τ_{ATM} and L_{FS} is acting as the free-space loss.

The free-space loss, for a certain wavelength λ at a certain distance d, is defined as follows:

$$L_{FS} = \left(\frac{\lambda}{4\pi d}\right)^2 \tag{2.2}$$

7

The gain of the transmitter G_T can be described as follows:

$$G_T = \frac{16}{\theta_T^2} \qquad (2.3)$$

Where θ_T is the full transmitting divergence angle. The gain of the receiver G_R, for a certain wavelength λ and a certain receiver diameter D, can be computed as follows:

$$G_R = \left(\frac{\pi D}{\lambda}\right)^2 \qquad (2.4)$$

τ_{ATM} can be described, using the atmospheric attenuation factor α and a certain distance d, as follows:

$$\tau_{ATM} = 10^{-\alpha d/10} \qquad (2.5)$$

If we insert now L_{FS}, G_T, G_R and τ_{ATM} in equation (2.1) described above, we end up with the following link budget calculation of the received power P_R:

$$P_R = P_T \left(\frac{D}{\theta_T d}\right)^2 \tau_T \cdot \tau_R \cdot 10^{-\alpha d/10} \qquad (2.6)$$

2.2 Atmospheric effects

The optical link quality in FSO systems is subject to different atmospheric effects. In the following sections the degree of attenuation on precipitation, fog, clouds, atmospheric turbulences and other effects is discussed.

2.2.1 Fog

The water droplet diameter in fog or haze is around $1\mu m - 15\mu m$, which is similar to the common optical wavelengths ($850nm - 1550nm$). Hence, Mie scattering leads to large attenuation of the optical signal. This is why fog or haze situations are responsible for the most attenuation on optical channels. The attenuation magnitude can rise up to 300 db/km in fog environments [14]. However, this largely depends on the local climate. The
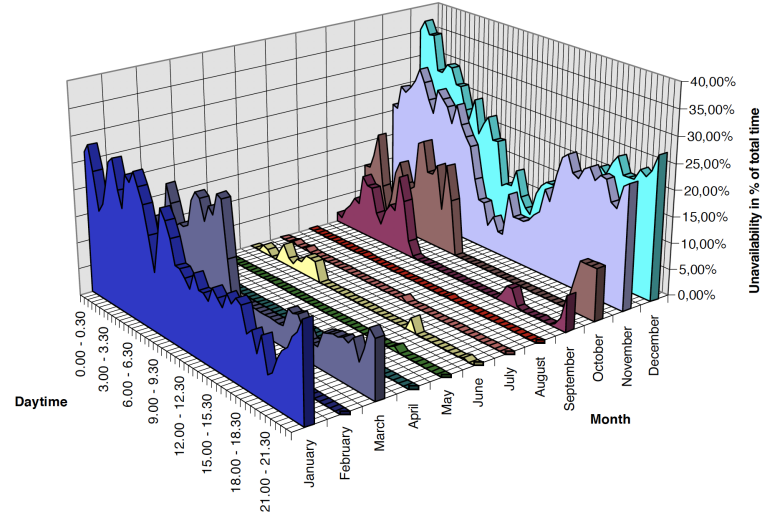
Figure 2.3: Unavailability w.r.t. daytime and month measured in Graz [14]

measurements by Leitgeb et al. (2003) [14] in figure 2.3 show that the the link unavailability increases in the foggy months (January, Februrary, November, December) in Graz, Austria. Especially at daytimes with a high probability for fog (early morning, late evening).

2.2.2 Precipitation

The attenuation of the optical link during precipitation events, like rain or snowfall, is comparably low compared to fog or haze. For high rain rates at 2 mm/min an attenuation of 15 db/km was measured for a wavelength of $\lambda = 850nm$ in Soni et al. (2017) [15]. Also the attenuation due to precipitation is dependent on the wavelength. Higher FSO wavelengths lead to higher attenuation. However, when it comes to fog, the wavelength dependence in attenuation is marginal [11].
Also heavy rain can cause FSO link interruption, especially in tropical environments with high humidity and hazy weather in general [16].

2.2.3 Clouds

When it comes to groud-to-space FSO links, also clouds have a large impact on the attenuation of the optical signal. The attenuation effects to optical signals is similar to fog. Different cloud types attenuates the FSO signal differently, due to the different sizes, water vapour densities and cloud concentrations (see figure 2.4). Rammprasath et al. (2013) [17] compared the cloud attenuation coefficient for different wavelengths and three different cloud types (cumulus, stratus and stratocumulus). The simulation results show that the optical signal is attenuated the most while propagating through stratocumulus clouds. The cumulus cloud attenuates the signal the least. The attenuation coefficient is between 38 dB/km (cumulus) and 52 dB/km (stratocumulus), depending on the cloud type, according to the simulation results of Rammprasath et al. (2013) [17].

2.2.4 Atmospheric turbulences

Atmospheric turbulences arise, due to variations of the refractive index of the atmosphere. If an optical signal propagates through the turbulent atmosphere, this can lead to beam wandering, scintillation or loss of spacial coherence [18], due to the fluctuations of the refractive index profile of the atmosphere. To cope with these fluctuations of the refractive index, different mathematical models exist to perform simulations in order to design an FSO system that meets the Quality of Service (QoS) parameters. The Hufnagel-Valley model is the most popular model to estimate the refractive index structure parameter profile $C_n^2(h)$.

The Hufnagel-Valley model is given as follows [19]:

$$
\begin{aligned}
C_n^2(h) = &0.00594 \left(\frac{v_{rms}}{27}\right)^2 \left(10^{-5} \cdot h\right)^{10} e^{-\frac{h}{1000}} + 2.7 \cdot 10^{-16} \cdot e^{-\frac{h}{1500}} \\
&+ A \cdot e^{-\frac{h}{100}}
\end{aligned}
\tag{2.7}
$$

A denotes the nominal value of the refractive index structure parameter at sea level and is often set to $A = 1.7 \cdot 10^{-13} m^{-2/3}$ for daytime conditions or $A = 1.7 \cdot 10^{-14} m^{-2/3}$ for nighttime conditions [19].
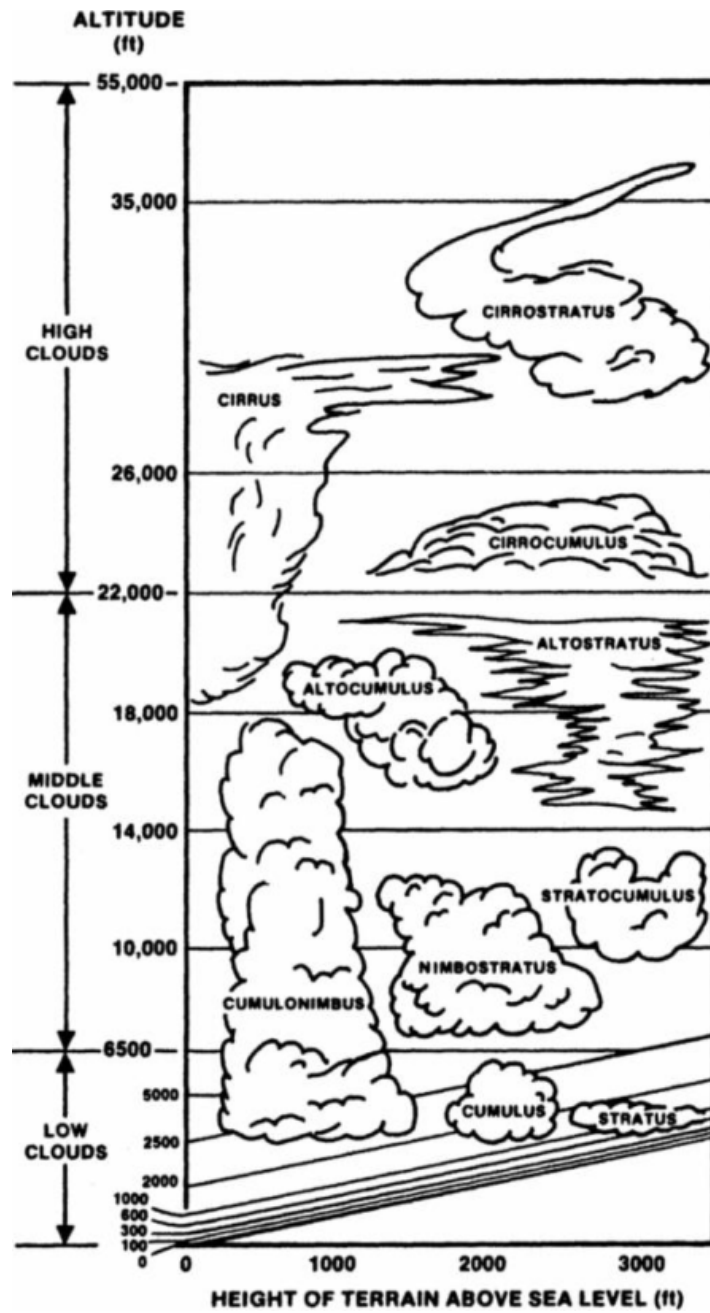
Figure 2.4: Different clouds with respect to different heights [17]

The Bufton wind model [19] is often used to approximate the wind wave profile of the atmosphere as follows:

$$v_{rms} = \left[\frac{1}{15 \cdot 10^3} \int_{5 \cdot 10^3}^{20 \cdot 10^3} \left(v_{wind} + v_T \cdot \exp\left\{ -\left(\frac{h - h_T}{d_T}\right)^2 \right\} \right)^2 dh \right]^{1/2}$$

(2.8)

With v_{wind} as the wind speed at ground level in (m/s), v_T as the wind speed at the tropopause in (m/s), h_T as the height of the tropopause in (m), and d_T as the thickness of the tropopause in (m).

Figure 2.5 shows the Hufnagel-Valley model for daytime and nighttime conditions, using the following parameters:

$$v_{wind} = 8.3 m/s$$
$$v_T = 25.28 m/s$$
$$h_T = 12000 m$$
$$h_T = 1000 m$$
$$A_{day} = 1.7 \cdot 10^{-13} m^{-2/3}$$
$$A_{night} = 1.7 \cdot 10^{-14} m^{-2/3}$$

Atmospheric turbulence models try to fit a mathematical model to the real refractive index profile. Since this is a regression task, also artificial neural networks can be used to create such models as proposed in [20]. A residual neural network (ResNet) was trained with data generated from the Hufnagel-Valey model using a measured wind profile, obtained RAwinsonde OBservation (RAOB) measurements from four different locations on earth. The results shown in 2.6 are using data from Güímar-Tenerife (ESP) captured on 10th March 2020 and give a promising outlook onto modelling the refractive index structure parameter with artificial neural networks or more specifically ResNets.
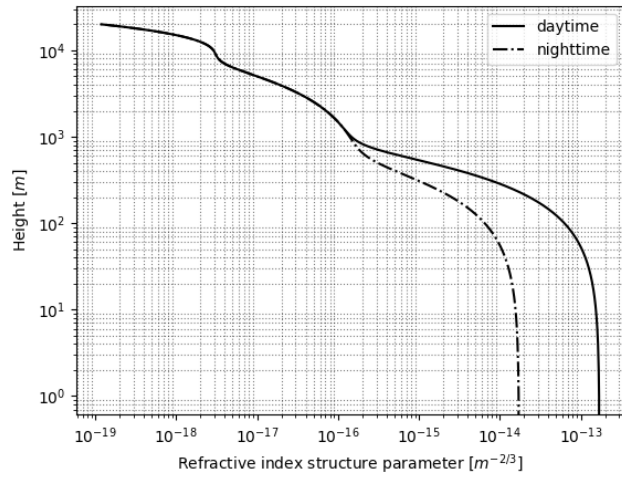
Figure 2.5: Hufnagel-Valley model for daytime and nighttime conditions
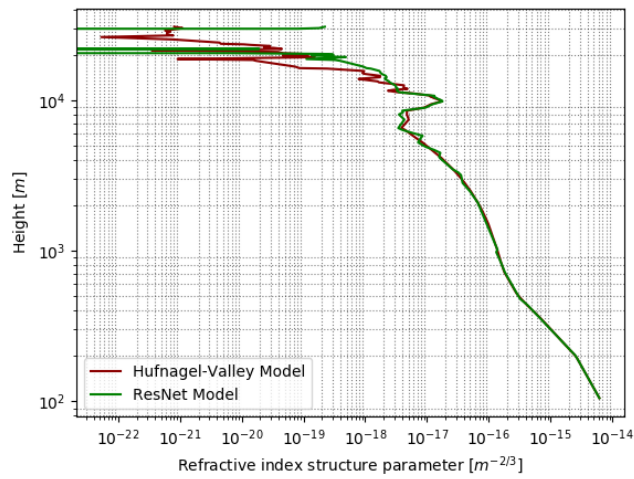
Figure 2.6: Hufnagel-Valley model vs. ResNet model [20]

2.2.5 Sandstorms

Not only rain, fog or clouds weaken the optical signal strength, but also sandstorms attenuate the optical wave as the results in Ghassemlooy et al. (2013) [21] show. The received optical power dropped by more than 6dB in sand conditions compared to clear sky conditions in the sandstorm chamber, under laboratory conditions. Due, to the size of the particles, the attenuation effect during sandstorms are comparable to fog events. However, the duration of sandstorm events is usually not as long as for fog events.

2.3 Optical fibres

Data in an optical domain can either be transmitted over free space or fibres. Fibres have the advantage that the light rays are guided, unlike FSO communication where a direct line of sight is necessary.

2.3.1 Physical structure

The physical structure of an optical fibre (see figure 2.7) consists of an inner core, where the light is propagating. The inner core is surrounded by a cladding, which prevents the light from exiting the core due to total reflection. The core and the cladding are made out of glass or plastic material. In order to trap the light inside the fibre, the refractive index of the core must be higher than the refractive index of the cladding. Only if this condition is given, the principle of total reflection applies and the light is trapped inside the core of the fibre. The coating is usually made out of plastic material and protects the cladding and the core from physical damage. To add additional strength and protection from physical stress, the coating is surrounded by a strength material like Kevlar. And the outer layer of the fibre is the jacket, which is mostly made out of plastic material. It provides additional strength and protection to the fibre.
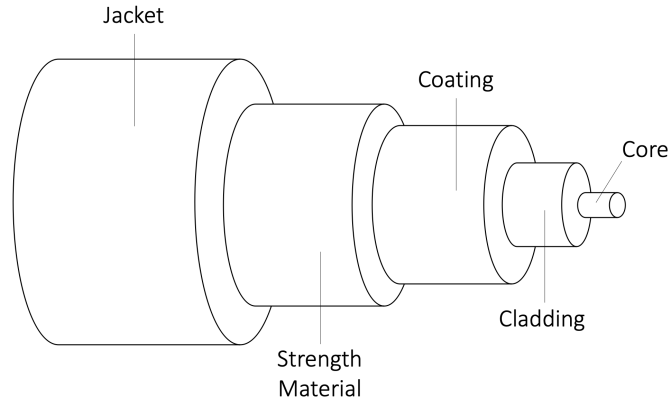
Figure 2.7: Optical fibre structure

2.3.2 Principle of total reflection

The light rays are trapped inside the fibre core due to the principle of total reflection. If a light ray is larger than a specific angle θ_{total}, then the light ray is completely reflected by the boundary between the cladding and the core (see figure 2.8). To compute the minimum angle θ_{total} of a light ray in order that total reflection happens, we make use of Snell's law.

Snell's law is given as follows:

$$n_1 \cdot \sin \theta_1 = n_2 \cdot \sin \theta_2 \tag{2.9}$$

In order to compute θ_{total}, the reflected angle θ_2 needs to be set to $\theta_2 = 90°$. With $\sin 90° = 1$ we get the following:

$$n_1 \cdot \sin \theta_{total} = n_2 \tag{2.10}$$

$$\sin \theta_{total} = \frac{n_2}{n_1} \tag{2.11}$$

$$\theta_{total} = \arcsin \left(\frac{n_2}{n_1} \right) \tag{2.12}$$

In order that total reflection happens, the following condition needs to be given: $n_1 > n_2$

Otherwise, total reflection would not be possible. This can be seen in equa-
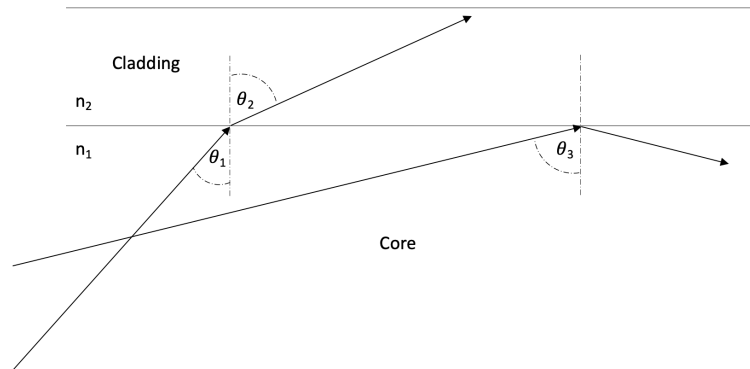
Figure 2.8: Refraction of light rays in an optical fibre core

tion (2.11), where $\sin \theta_{total}$ would be bigger than 1, which is impossible.

In figure 2.8 we have two light rays with different incoming angles θ_1 and θ_3. The incoming angle of the first light ray is smaller than the minimum angle of total reflection ($\theta_1 < \theta_{total}$). Hence, the light ray is not reflected, but propagates further into the cladding of the fibre. The second light ray is less steep than the first one, with an incoming angle larger than the minimum angle of total reflection ($\theta_2 > \theta_{total}$). This light ray is completely reflected by the boundary layer between the cladding and the core of the fibre and propagates further through the core of the fibre.

2.3.3 Single mode fibres

Single mode fibres, as the name suggests, only supports a single mode. This is due to the small core diameter, which is usually between $8\mu m$ to $10\mu m$. Only one light ray is propagating through the core of the fibre, which has the advantage that no dispersion effects occur. Very high data rates can be achieved, due to the lack of dispersion at the end of the fibre. Thus, theoretically an unlimited bandwidth is supported. The attenuation in single mode fibres is very low ($< 1dB/km$), because only one ray of light propagates through the fibre resulting in low internal reflections and thus low attenuation. Therefore, data can be transmitted over high distances,

due to the low attenuation of the fibre. Single mode fibres are usually specified for a specific wavelength or a very narrow range of wavelengths.

2.3.4 Multi mode fibres

Multi mode fibres support the propagation of multiple modes simultaneously. The core diameter is typically between $50\mu m$ to $100\mu m$, which leads to multiple light rays propagating through the core of the fibre. As a result, dispersion effects occur, which limit the bandwidth and data rate. A lager diameter of the fibre core leads to more modes propagating through the fibre. More modes also imply more internal reflection which results in a higher attenuation compared to single mode fibres. Hence, multi mode fibres are mostly used for short distances (for example in local area networks), due to the larger attenuation. Multi mode fibres are usually specified for a wide range of wavelengths.

2.4 Signal generation and modulation

Like in every other telecommunication system the data needs to be modulated on a carrier wave in order to transmit information between two entities. In optical communication typically two modulation schemes are very popular. On-off keying and pulse position modulation. Both modulation schemes modulate the amplitude of the carrier wave to a 100%. This can either be done by modulating the laser diode directly (internal modulation) or by attaching a dedicated modulator to the laser diode (external modulation) which modulates the amplitude.

2.4.1 On-off keying

The simplest method of modulating data onto a carrier wave is on-off keying (OOK) which is, in some literature, denoted as non-return-to-zero (NRZ) code. Using OOK, the carrier wave is simply just turned on and off, as the name suggests. A logical **1** is represented by the carrier wave turned on and a logical **0** is represented by the carrier wave turned off (see figure 2.9). The input signal can be used to modulate the laser diode directly or it can be fed directly into the external modulator, which makes this
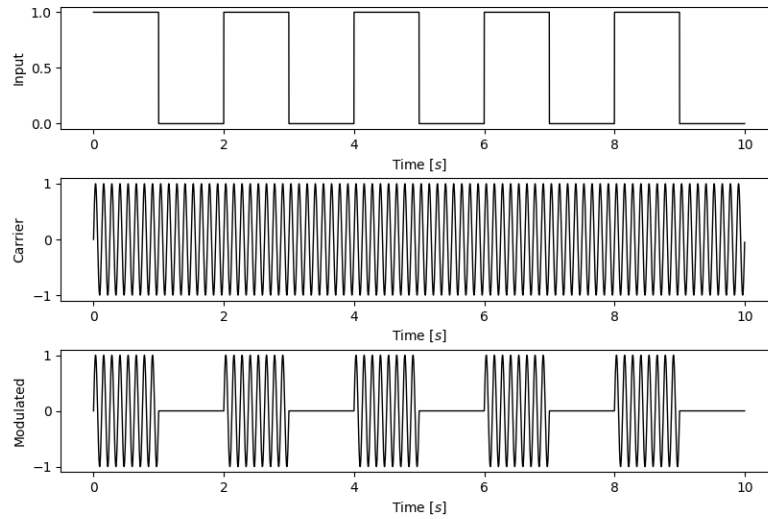
Figure 2.9: OOK modulation scheme. Input signal (top), carrier wave signal (middle), modulated signal (bottom)

modulation scheme very convenient and simple. Due to the simplicity, the bandwidth efficiency and the low cost, this modulation scheme is used the most, especially in FSO systems.

2.4.2 Pulse position modulation

Pulse position modulation (PPM) also modulates the amplitude similar to OOK. However, only a single short pulse encodes a complete symbol of multiple bits, which makes this modulation scheme very energy efficient. All pulses have the same amplitude and the same pulse width. The data is encoded in the position of the pulse relative to a clock signal. This also induces a synchronisation problem. The clocks of the transmitter and the receiver must be perfectly synchronized in order to decode the signal and extract the data. Therefore, mostly differential pulse position modulation is used, where each pulse position is placed relative to the previous pulse. This makes it easier for the receiver to decode the signal, since only the time difference of two pulses need to be measured and no clock signal is needed. An example of a pulse encoding of different symbols is shown in

figure 2.10. Each symbol consists of two logical bits and is encoded using a pulse with a different timing behaviour relative to a clock signal. In figure 2.11 multiple symbols are transmitted and the resulting pulse train, using the encoding from figure 2.10, can be observed. With one pulse, multiple bits of data can be transmitted. Hence, the transmission efficiency is higher compared to OOK [22]. Besides of that it is also very energy efficient, due to the short pulses. On the other hand, PPM is very sensitive to interferences, which leads to bit errors at the other end of the transmission channel. Especially in wired copper connections the system has to deal with external influences. However, in optical communication systems, external influences and interferences are not so much of a problem, due to the properties of light. This makes PPM very suitable for optical communication systems.
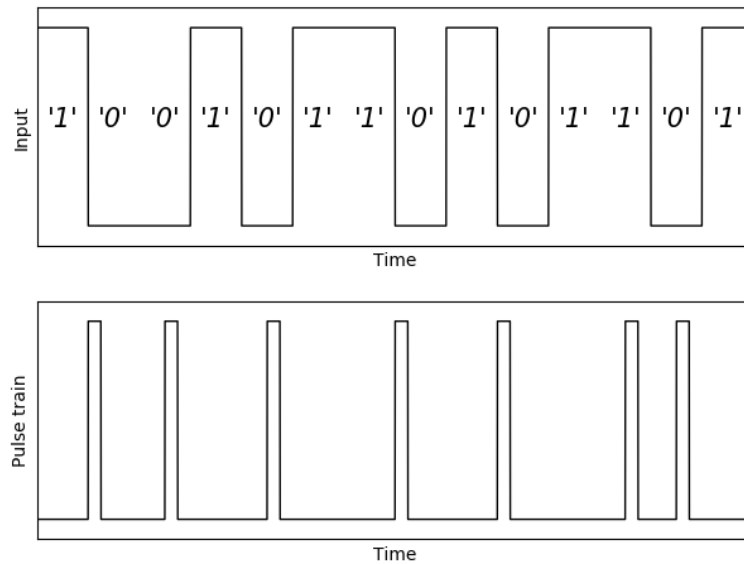
Figure 2.11: Pulse train of a PPM modulated input signal

Given the number of PPM slots L, the power requirement is approximately

(a) Pulse encoded symbol '00'

(b) Pulse encoded symbol '01'

(c) Pulse encoded symbol '10'

(d) Pulse encoded symbol '11'
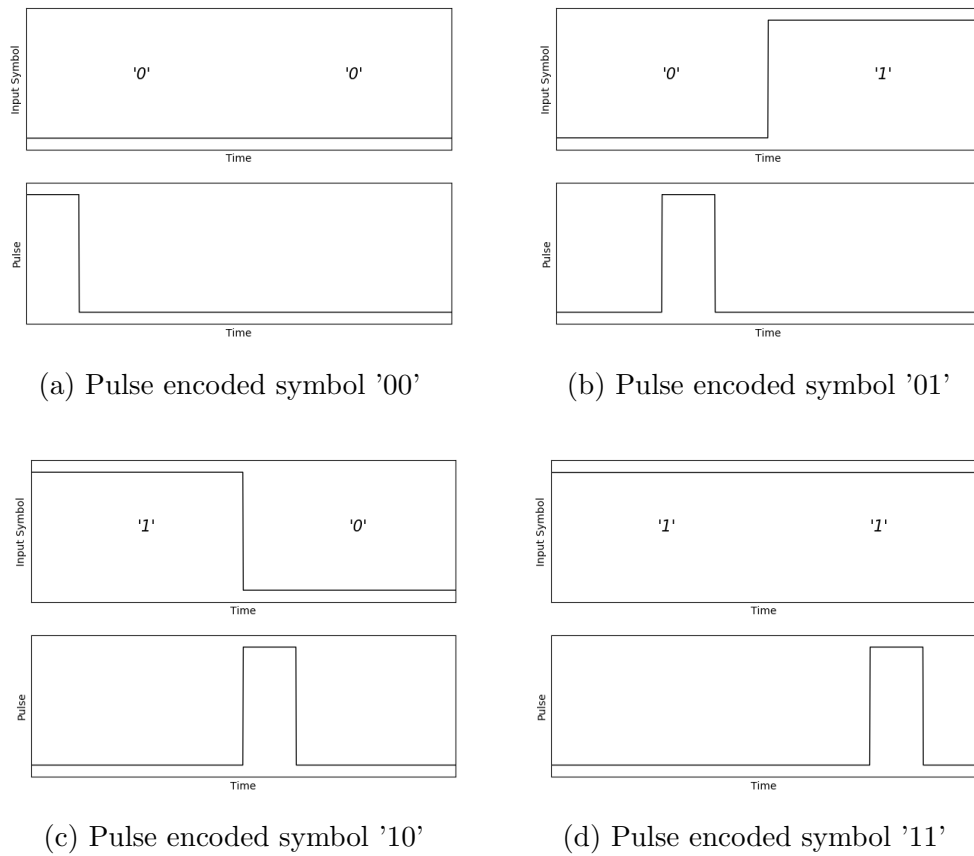
Figure 2.10: Example PPM encoding of different symbols

[23]:

$$\frac{P_{PPM}}{P_{OOK}} \approx \sqrt{\frac{2}{L \log_2 L}} \tag{2.13}$$

The bandwidth which is required to obtain the bit rate R_b is described as follows [23]:

$$B = \frac{L \cdot R_b}{\log_2 L} \tag{2.14}$$

In equation 2.13 it can be seen that the PPM modulation requires less power compared to OOK, if the number of slots L is greater than 2. Which is expected, due to the short pulse duration. However, besides the complexity of PPM and its implementation, PPM modulation also suffers from bandwidth expansion, since a higher level of accuracy is needed in slot synchronization [24]. In equation 2.14 it can be observed, that a higher bandwidth is required to obtain a certain bit rate R_b, if more PPM slots are used. Optical communication systems typically have a high bandwidth which makes PPM an excellent choice for FSO communication. Since PPM modulation schemes are very power efficient, also the bit error rate (BER) performance is increased compared to OOK [25]. Hence, a lower signal to noise ratio (SNR) is needed for PPM to achieve the same BER as OOK.

3 System design

The following chapter describes the proposed model architecture of the Optical Ethernet Transceiver Modem. First a theoretical overview is given, followed by the description of the physical components which are used for the system and later on the measurements.

3.1 Architecture

The system architecture of the Optical Ethernet Transceiver Modem (OETM) in figure 3.1 allows a bidirectional transmission of optical signals and electrical signals (Ethernet). Given an optical input signal, the data can be transmitted over Ethernet and the optical output directly. A given Ethernet input is transformed into an optical output signal and also an Ethernet output. This also applies on the receiving side of the transmitter modem, due to the bidirectional system design.

To make a bidirectional transmission possible, optical fibre couplers are used. One fibre coupler is used for the transmitting side of the modem and another fibre coupler is used for the receiving side of the modem. Hence, the transmitting part on one side of the optical Ethernet modem is split up into two paths, which are connected of the receiving Ethernet and optical part on the other side. The receiving part on one side of the modem is split up and connected to the transmitting Ethernet and optical part of the other side of the modem. However, only half of the signal power reaches the other side of the modem, since the signals are evenly split by the optical fibre couplers.

The conversion of the electrical Ethernet signals is done using media converters in combination with small form-factor pluggable (SFP) modules. This allows high data rates up to 1.25 Gbps and a reliable data transmission. Due to the common use of SFP modules in IP networks, the price of such a system is also very low.

The optical power needs to exceed a certain threshold level in order to decode the data in a reliable way and for minimizing the bit error rate. If the received optical power is too low, the signal can be amplified using an optical amplifier, such as an erbium doped fibre amplifier.
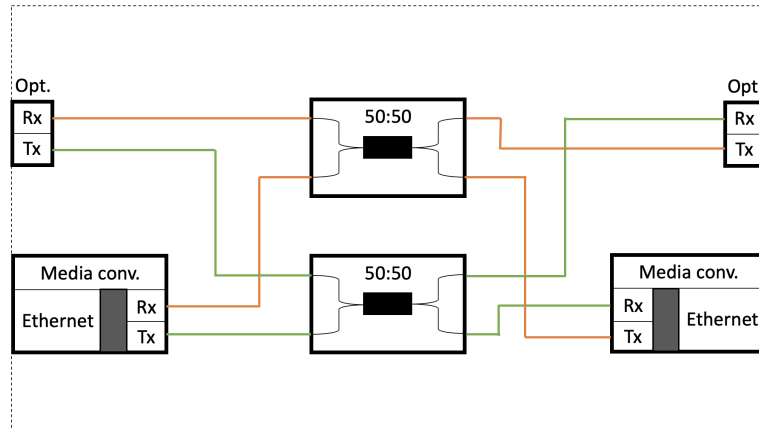
Figure 3.1: OETM system architecture

If bidirectional SFP modules are used, the system architecture is getting much simpler (see figure 3.2). Bidirectional SFP modules transmit data in both directions over one fibre channel using different wavelengths for the transmitting and the receiving signals. Hence, one optical fibre coupler can be spared which makes the overall system cheaper and more compact in size. Due to these advantages, the system architecture in figure 3.2 was chosen for the final design.
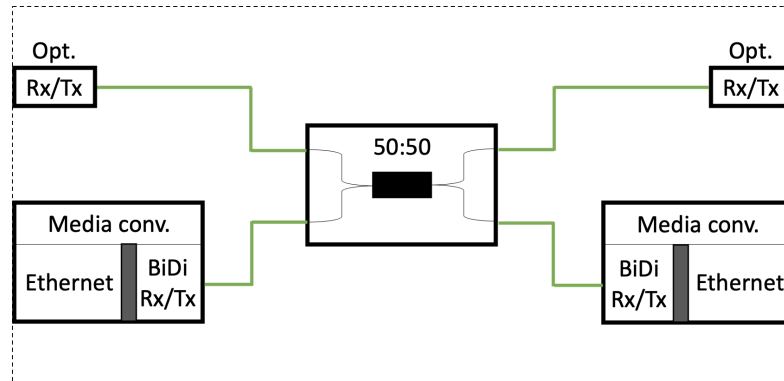
Figure 3.2: OETM system architecture using bidirectional SFP modules

3.2 Components

This section describes the components used for the Optical Ethernet Transceiver Modem (OETM). The corresponding datasheets can be found in Appendix B-E.

3.2.1 SFP modules

The interface from the electrical domain into the optical domain is maintained by the following SFP modules:

- 1000BASE-BX SFP Transceiver Module 1550nm/1490nm
- 1000BASE-BX SFP Transceiver Module 1490nm/1550nm

High data rates (1.25 Gbps), using wavelengths which provide eye safety for FSO communication, are supported by the selected SFP modules. Since the selected SFP modules are bidirectional, one optical fibre coupler can be spared. SFP modules are protocol transparent, meaning the digital differential input signal will be directly sent out on the optical interface and vice versa. Hence, the SFP modules transmit data regardless of the protocol used. The modulation scheme of the optical domain, using the selected SFP modules, is OOK.

1000BASE-BX SFP Transceiver Module 1550nm/1490nm

– Vendor Name: FS
– Compatibility: FS Genuine
– Bidirectional: Yes
– Maximum Data Rate Tx/Rx: 1250/1250Mbps
– Wavelength Tx/Rx: 1550nm/1490nm
– Maximum Cable Transmission Distance: 80km
– Coupled Fibre: Single Mode 9/125μm G.652
– Tx Power: -2dBm to 3dBm
– Rx Sensitivity: ¡ -24dBm
– Receiver Damage Threshold: ¿3dBm
– Connector: LC simplex
– Protocols: Fast Ethernet, Gigabit Fibre Channel, MSA Compliant

1000BASE-BX SFP Transceiver Module 1490nm/1550nm

– Vendor Name: FS
– Compatibility: FS Genuine
– Bidirectional: Yes
– Maximum Data Rate Tx/Rx: 1250/1250Mbps
– Wavelength Tx/Rx: 1490nm/1550nm
– Maximum Cable Transmission Distance: 80km
– Coupled Fibre: Single Mode 9/125μm G.652
– Tx Power: -2dBm to 3dBm
– Rx Sensitivity: ¡ -24dBm
– Receiver Damage Threshold: ¿3dBm
– Connector: LC simplex
– Protocols: Fast Ethernet, Gigabit Fibre Channel, MSA Compliant

Figure 3.3: FS 1000BASE-BX SFP Transceiver Module

3.2.2 Media converter

The Ethernet communication interface is handled using two media convert-
ers. The "Mini Gigabit Ethernet Media Converter, 1x 10/100/1000Base-T
RJ45 to 1x 1000Base-X SFP Slot" by the vendor FS (see figure 3.4) trans-
late the Ethernet frames into an electrical signal, which is further processed
by an SFP module. As a result of this, an optical signal is obtained. Media
converters are usually used to enable optical network communication in an
existing Ethernet infrastructure. Since the vendor of the chosen media con-
verter is FS, the corresponding SFP modules also need to be FS compatible
to provide a working communication between the Ethernet interface and
the SFP module on the electrical domain. In figure 3.5 the interface usage
of the media converter is described. A SFP module is plugged into the SFP
slot of the media converter. To further transmit the optical signal a LC-LC
duplex single mode fibre patch lead is connected to the SFP module. In
the Ethernet slot of the media converter an Ethernet patch cable (typically
CAT5) can be directly connected.

Figure 3.4: FS Mini Gigabit Ethernet Media Converter
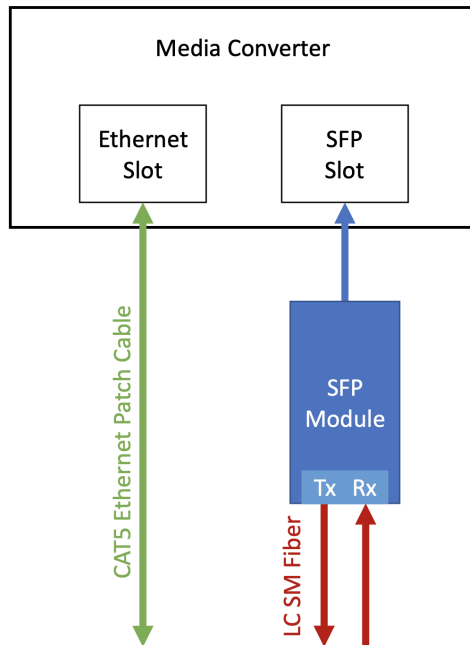
Figure 3.5: Media converter interface usage

27

3.2.3 Optical fibre coupler

To split optical signals, the *Thorlabs BXC15 - 2x2 Boxed Wideband Fibre Optic Coupler* (see figure 3.6) is used. The coupler supports wavelengths of 1550nm $\pm$ 100nm with an excess loss $L_{excess,dB} \leq 0.15dB$, which is sufficient for the used SFP modules. The excess loss is denoted in equation 3.1. The rugged casing of the coupler protects the inside, which are mostly fragile fibre components, and is therefore ideal for laboratory environments. Since the coupler comes with FC/APC bulkheads, a LC to FC adapter is needed in order to connect the coupler to the optical output of the SFP modules. The coupling ratio is 50:50, which means only half the power is received at the signal output and the tap output, due to the splitting of the signal.

The excess loss is the ratio of the input power to the total output power:

$$L_{excess,dB} = 10 \log \frac{P_{input,mW}}{P_{port3,mW} + P_{port4,mW}} \tag{3.1}$$

The loss due to polarisation is the ratio of the maximum transmitted power to the minimum transmitted power.

$$L_{polarization,dB} = 10 \log \frac{P_{max,mW}}{P_{min,mW}} \tag{3.2}$$

The optical return loss is the ratio of the input power at port 1 to the input power at port 2. The output is due to the back reflection of the junction of the coupler.

$$L_{return,dB} = 10 \log \frac{P_{port1,mW}}{P_{port2,mW}} \tag{3.3}$$

The insertion loss is the ratio of the input power at one of the two inputs to the output power at one of the two outputs.

$$L_{insertion,dB} = 10 \log \frac{P_{input,mW}}{P_{output,mW}} \tag{3.4}$$

Figure 3.6: Thorlabs BXC15 - 2x2 Boxed Wideband Fibre Optic Coupler

3.2.4 Fibres

Since the fibre optic coupler is using single mode fibres, also single mode fibres need to be used for the connections between the SFP modules and the fibre coupler. Otherwise, a lot of signal power is lost, due to the different core diameters of multi mode fibres and single mode fibres. However, the signal power only degrades, if an optical signal is coupled from a mono mode fibre into a single mode fibre (see figure 3.7). Parts of the signal will be coupled into the cladding of the single mode fibre and the signal does not reach the other side of the fibre. Therefore, only single mode fibres are used in this system.
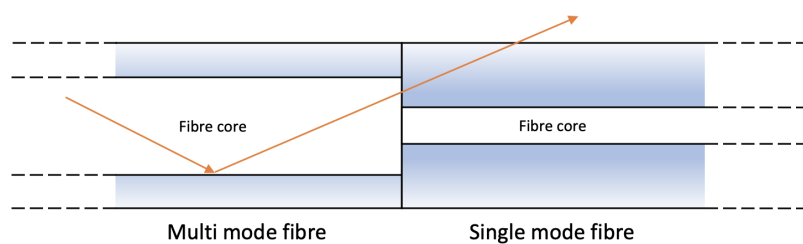
Figure 3.7: Signal loss, due to mono mode to single mode fibre coupling

4 Measurement results

This chapter covers the measurements of the Optical Ethernet Transceiver Modem. In the first measurement, the Ethernet-to-Ethernet connection is analysed, the bit rate measured and compared with the direct Ethernet link. The second measurement analyses the Ethernet-to-Optical connection and the third measurement analyses the Optical-to-Ethernet connection of the transceiver modem.

4.1 Bit rate measurement

To estimate the bit rate of the Optical Ethernet Transceiver Modem (OETM), the measurement setup in figure 4.1 is used. Data is transmitted from one PC to another PC, which are directly connected over the transceiver modem, using a software written in $C++$. The software is sending transmission control protocol (TCP) frames to estimate the overall bit rate of the complete system (including the PCs). It is expected that the bit rate is much lower than 1.25 Gbps, due to the delays induced by the PCs and its hardware interfaces, such as:

- **Queuing delay:** Is the time a frame is spending on a hardware queue buffer (ingress and egress).
- **Serialization delay:** Is the time to send all bits from the hardware buffer onto the physical medium.
- **Propagation delay:** Is the time for a frame to reach the destination of the physical medium.
- **Software delay:** Is the time for a frame to be processed by the software.
- **Scheduling delay:** Is the time the software is not active, due to task scheduling of the operating system.
- **Fragmentation delay:** Is the fragmentation overhead of the network stack, in order to transmit large amounts of data.

These delays occur on every hardware interface of the PCs, SFP modules, media converters and physical connections. Hence, the overall bit rate will be lower than 1.25 Gbps even though the individual parts are designed for a bit rate of 1.25 Gbps.

To measure the overall bit rate, a time stamp is transmitted in the first frame. After that a constant bit stream is sent over the transceiver modem. At the receiver side, the overall bit rate can be measured using the time stamp which was sent by the transmitter at the beginning, the time stamp of the latest received frame and the number of bits which are received in total, using the following formula:

$$BR = \frac{N_{received}}{t_{last} - t_{first}} \tag{4.1}$$

With $N_{received}$ denotes the number of bits which are received. t_{last} is the time at which the last frame was received and t_{first} at which the first frame was sent by the transmitting PC.

4.1.1 Measurement setup

Figure 4.1 shows the measurement setup for estimating the bit rate of the OETM using two PC endpoints. Within the OETM, the Ethernet signals are translated into optical signals and back to Ethernet signals for this setup.
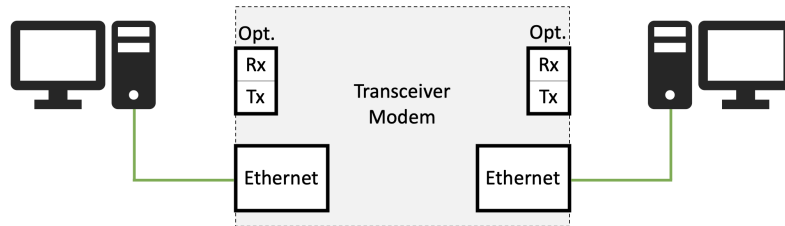
Figure 4.1: Measurement setup for bit rate measurement

Devices used:

- **PC 1:** HP - Inv. Nr.: 177727 (Transmitter)
- **PC 2:** Lenovo - Inv. Nr.: 0184208 (Receiver)
- **Media Converter:** FS - Mini Media Converter MMC-GASFP-V 1000Base-X
- **SFP module 1:** FS - 1000BASE-BX SFP Transceiver Module 1550nm/1490nm
- **SFP module 2:** FS - 1000BASE-BX SFP Transceiver Module 1490nm/1550nm
- **Ethernet cable:** Cat6a Snagless SFTP PVC Patch Cable
- **Optical fibre:** 9/125 Single Mode Fibre Patch Cable-1M

4.1.2 Measurement software

The software which is used to estimate the bit rate, consists of two parts. A transmitter software and a receiver software which are executed on the two PCs respectively. Hence, one PC acts as a transmitter and the other PC acts as a receiver. The bit rate is computed using the amount of the transmitted data with respect to the time which is needed for the transmission. Since TCP is used for data transmission, a socket connection needs to be established between the transmitter and the receiver software. Due to the direct connection of the PCs, no IP address is assigned by default. Hence, a static IP address needs to be configured on both hosts, in order to be able to establish a socket connection. The sequence used for bit rate estimation is shown in figure 4.2. The individual software parts are described down below.

Transmitter software

At the beginning the transmitter software (see figure 4.3) opens a socket connection in listening state. Hence, the transmitter software acts as a server. Once the receiver software connects to the transmitter socket, the data is exchanged. First the transmitter software is sending out a time stamp, in order to keep track of the total transmission time. The time stamp is an unsigned integer value which translates into four bytes of payload. After the time stamp is sent, the main transmission of the data begins. For

32
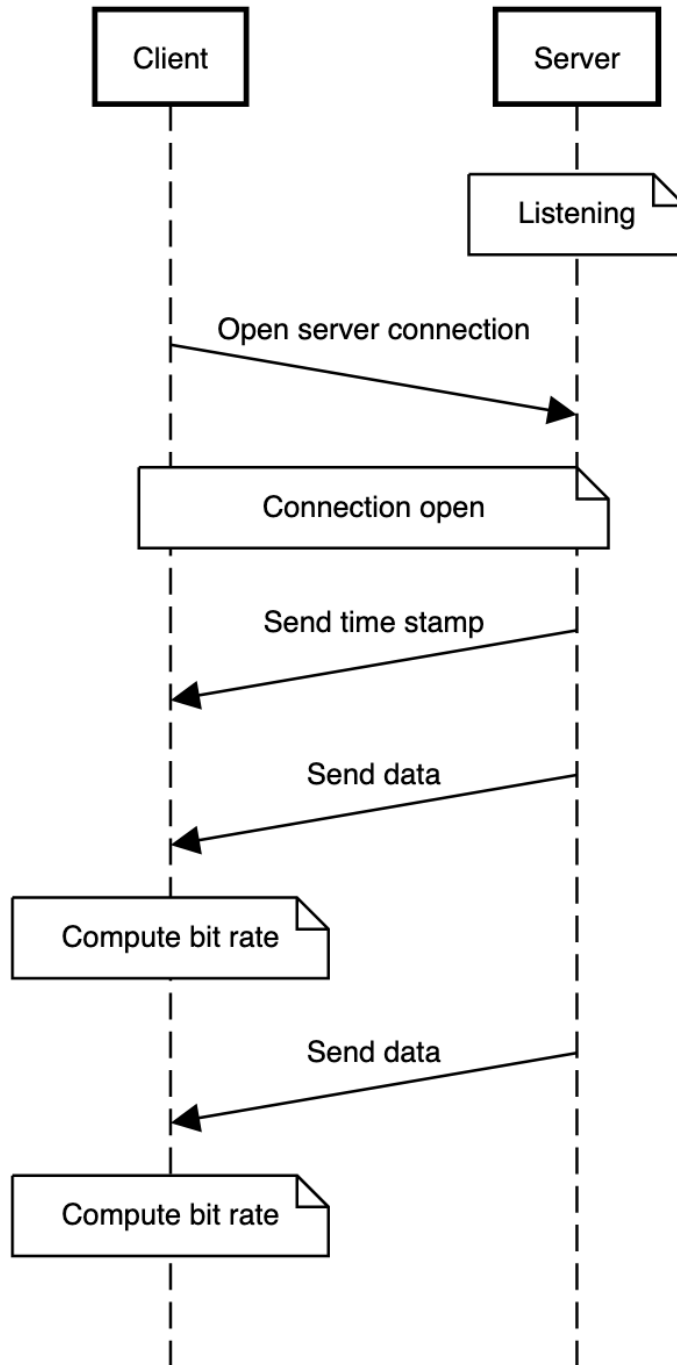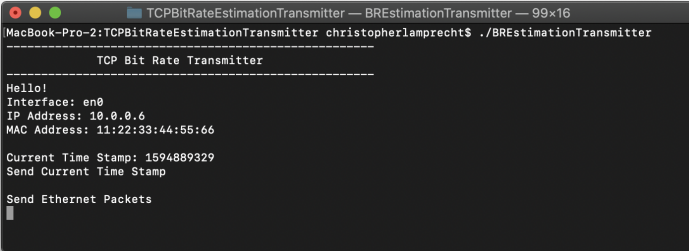
Figure 4.2: Sequence diagram for bit rate estimation

this the payload size of 500000 bytes is used and filled with random data. In order to save computing power and time, the same frame is sent over and over again. The network is flooded with these packets as fast as possible in order to achieve high bit rates.
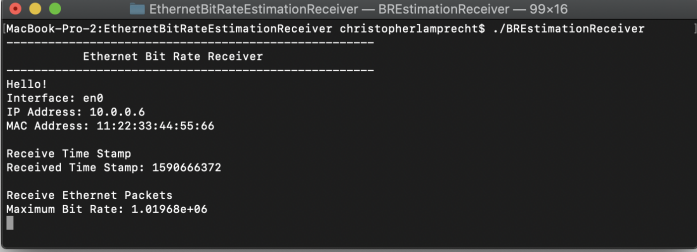
Figure 4.3: Transmitter software used for the bit rate estimation

Note: The MAC address is censored in figure 4.3, due to privacy reasons.

Receiver software

The receiver software (see figure 4.4) connects to the socket, which is opened by the transmitter software and waits for the incoming time stamp of the transmitting PC. After the time stamp is received, the packet flood of the transmitter is received and the bits are counted. With each packet received, the bit rate is computed and stored. After some time the bit rate converges to a maximum value and the final value is printed on the console output.

Figure 4.4: Receiver software used for the bit rate estimation
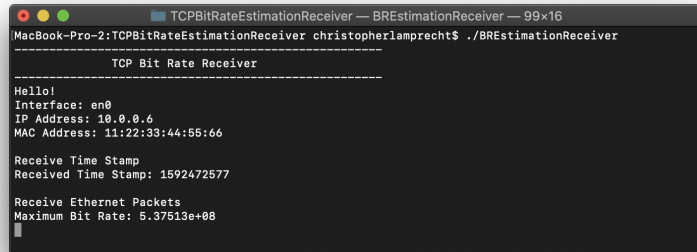
Note: The MAC address is censored in figure 4.4, due to privacy reasons, and the maximum bit rate result shown is only for demonstration purposes and not the final measured bit rate.

4.1.3 Results and discussion

All measurement results for this measurement setup are listed in the Appendix A. Figure 4.5 shows the final bit rate measurement results using the OETM. A bit rate of 537.51 Mbps could be measured at maximum. 100 measurements have been performed and the average bit rate, which was achieved, is 489.13 Mbps with a standard deviation of 38.09 Mbps.

Figure 4.6 shows the final bit rate measurement results using a direct Ethernet link between the two hosts. A bit rate of 536.32 Mbps could be measured at maximum. 100 measurements have been performed and the average bit rate, which was achieved, is 495.13 Mbps with a standard deviation of 39.19 Mbps.
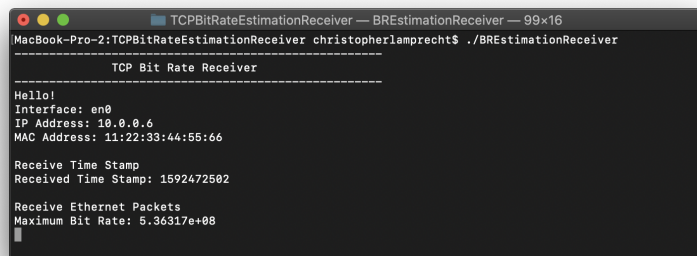
Figure 4.5: Results of the bit rate measurement using the OETM

Figure 4.6: Results of the bit rate measurement with direct Ethernet link

Note: The MAC address is censored in figure 4.5 and 4.6, due to privacy reasons.

As expected, we could not achieve a bit rate in the gigabit range, due to the delays described in the introduction. An average bit rate of 489.13 Mbps can be measured over the full communications channel including the hosts with the OETM and a bit rate of 495.13 Mbps can be measured on average with a direct link connection over Ethernet between the two hosts. The measured bit rate of the direct connection is a bit higher, as if the OETM is used, because the transceiver modem translates the Ethernet

frames into optical signals and back to Ethernet frames again which leads to larger delays. Thus, a lower bit rate is achieved on average with the OETM. However, the difference is not too large and the maximum bit rate can still be higher with OETM compared to the direct Ethernet link, which can be observed in the measurements.

4.2 Evaluation of the optical path

The measurement setup, shown in figure 4.7, is used to evaluate the received bit stream on the optical domain of the transmitter modem. A $C++$ software is used to transmit data over the Ethernet domain. The media converter in combination with an SFP module inside the transceiver modem, translates the Ethernet frame into an optical signal which is then passed to the optical output of the transceiver modem. The optical signal is then translated into an electrical signal, using a SFP module in combination with a SFP breakout board. The obtained electrical signal is later on measured with an oscilloscope. It is expected that the measured optical signal is consistent with the Ethernet frame, sent out by the PC.

4.2.1 Measurement setup

Figure 4.7 shows the measurement setup for evaluating the optical communications path on the receiver side using a SFP module in combination with a SFP breakout board. The translated electrical signal by the SFP breakout board is then measured using an oscilloscope.

Figure 4.7: Measurement setup for evaluating the optical path

Devices used:

- **PC:** Lenovo - Inv. Nr.: 0184208 (Transmitter)
- **SFP Breakout Board:** Group14 Technologies - SFP+ Breakout SFP2SMA2 Inv. Nr.: 0184251
- **Oscilloscope:** Rohde&Schwarz RTO 1044 Oscilloscope 4GHz 20GSa/s Inv. Nr.: 0171972
- **Media Converter:** FS - Mini Media Converter MMC-GASFP-V 1000Base-X
- **SFP module 1:** FS - 1000BASE-BX SFP Transceiver Module 1550nm/1490nm
- **SFP module 2:** FS - 1000BASE-BX SFP Transceiver Module 1490nm/1550nm
- **Ethernet cable:** Cat6a Snagless SFTP PVC Patch Cable
- **Optical fibre:** 9/125 Single Mode Fibre Patch Cable-1M

4.2.2 Measurement software

The measurement software (see figure 4.10) for the evaluation of the optical output path is kept very simple. The same packet is transmitted over and over again. The data of the packet has a certain bit structure in order to distinguish the measurement data from the rest of the network traffic which is usually sent out by the hosts. Since the data is sent over Ethernet, the following frame structure is used:

Ethernet Frame			
Destination MAC	Source MAC	Ethertype	Payload
6 Bytes	6 Bytes	2 Bytes	0-1500 Bytes

Figure 4.8: Ethernet frame structure

- **Destination MAC:** Denotes the MAC address of the host to which the frame is sent
- **Source MAC:** Denotes the MAC address of the host which is transmitting the frame
- **Ethertype:** Indicates the protocol type which is used in the payload

- **Payload:** Data which is transmitted

Due to the frame structure, a minimum frame size of 14 bits needs to be transmitted with a payload size of 0. The frame which is transmitted by the software is shown in figure 4.9. All values are hexadecimal.
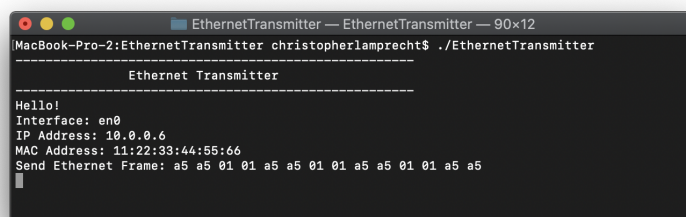
Ethernet Frame			
Destination MAC	Source MAC	Ethertype	Payload
0xA5, 0xA5, 0x01, 0x01, 0xA5, 0xA5	0x01, 0x01, 0xA5, 0xA5, 0x01, 0x01	0xA5, 0xA5	-

Figure 4.9: Data which is transmitted by the software.

The unique bit structure of this frame makes it very distinguishable from the rest of the network traffic. The bit structure which is transmitted is the following:

```
10100101 10100101 00000001 00000001 10100101 10100101 00000001
00000001 10100101 10100101 00000001 00000001 10100101 10100101
```

The frame starts and ends with a `1`, contains a consistent toggling of the bit state during `0xA5` is sent, followed by longer transmit pauses while `0x01` is transmitted. This bit pattern is expected to be visible on the oscilloscope.

Figure 4.10: Transmitter software used for the evaluation

Note: The MAC address is censored in figure 4.10, due to privacy reasons.

4.2.3 Results and discussion

The measurement of the received data from the SFP module are shown in figure 4.11. The analogue bandwidth of the oscilloscope used for the measurements is 4 GHz with a sample rate of 20 GSa/s, which is sufficient for the maximum data rate of the SFP modules of 1.25 Gbps.
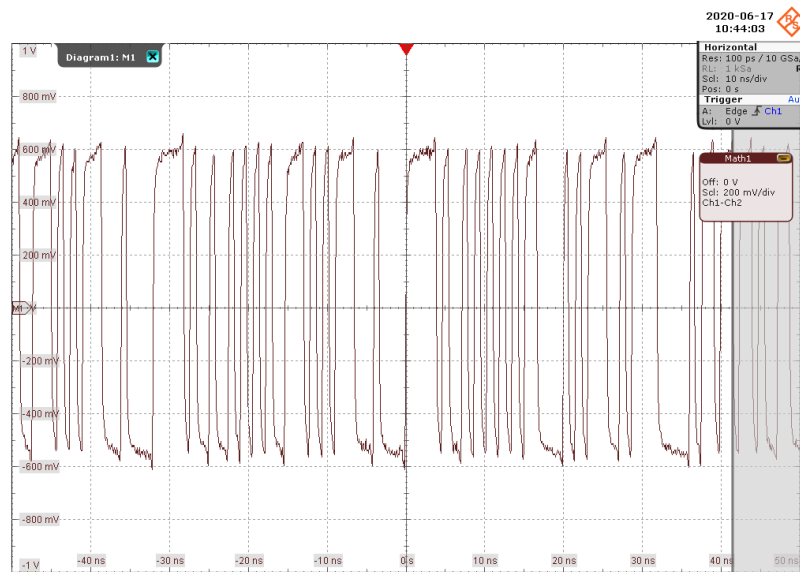
Figure 4.11: Received bit stream from the SFP module

The received bit stream can be observed in figure 4.11. This bit stream is not the same bit stream which was sent out by the PC. Hence, the data cannot be received using this method due to the properties of the media converter used. Usually Ethernet endpoints need to synchronize with each other in order to exchange the Ethernet frames. This is done using the Auto-Negotiation procedure. The measured bit stream refers to this Auto-Negotiation procedure and not to the sent bit stream. Hence, if a satellite uplink needs to be established, this Auto-Negotiation procedure needs to be implemented on the satellite side as well, in order to exchange data using this system.

Auto-Negotiation

Auto-Negotiation is used by two Ethernet endpoints in order to negotiate modes of operation, i.e. duplex mode. The procedure must be performed when the link is initially connected or a renegotiation request is made. The Auto-Negotiation procedure is specified in clause 37 in IEEE 802.3 [26] for 1000BASE-X Ethernet. Since the 1000BASE-X Ethernet media converter is operating at 1.25 Gbps, one code-bit has the duration of 0.8 ns, which is also compliant with the measurements shown in figure 4.11.

4.3 Evaluation of the Ethernet path

The Ethernet frames, translated from the optical signal, are evaluated in the measurement shown in figure 4.12. The importance of this measurement setup is very high, since mostly optical satellite signals are processed by the optical ground station. Hence, mostly optical signals are received and need to be translated into the Ethernet domain. The Ethernet frame, translated by the transceiver modem, is expected to be consistent with the received optical signal. The optical signal is generated by an SFP module in combination with the SFP breakout board. A high frequency signal is generated using a signal generator and fed into the SFP breakout board.

4.3.1 Measurement setup

Figure 4.12 shows the measurement setup for evaluating the Ethernet path on the receiver side using a PC endpoint. The optical signal is generated using a SFP module in combination with a SFP breakout board and a function generator.
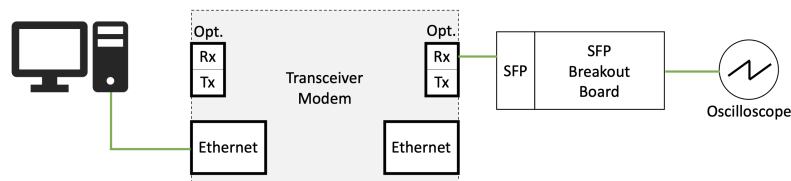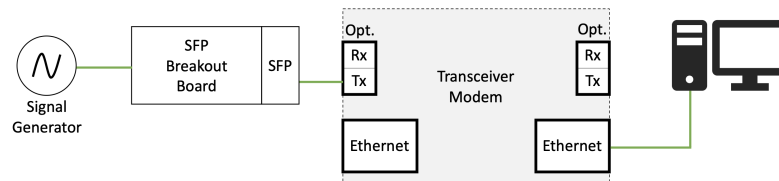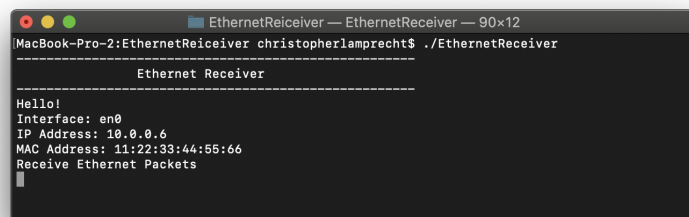

Figure 4.12: Measurement setup for evaluating the Ethernet path

Devices used:

- **PC:** Lenovo - Inv. Nr.: 0184208 (Transmitter)
- **Optical Signal Generator:** Agilent - 8164A Lighwave Measurement System Inv. Nr.: 0016076
- **Clock Signal Generator:** Agilent - N4906B 12.5 Gb/s BERT
- **SFP Breakout Board:** Group14 Technologies - SFP+ Breakout SFP2SMA2 Inv. Nr.: 0184251
- **Media Converter:** FS - Mini Media Converter MMC-GASFP-V 1000Base-X
- **SFP module 1:** FS - 1000BASE-BX SFP Transceiver Module 1550nm/1490nm
- **SFP module 2:** FS - 1000BASE-BX SFP Transceiver Module 1490nm/1550nm
- **Ethernet cable:** Cat6a Snagless SFTP PVC Patch Cable
- **Optical fibre:** 9/125 Single Mode Fibre Patch Cable-1M

4.3.2 Measurement software

The measurement software (see figure 4.13) for the evaluation of the optical input path is kept very simple. The software is waiting for packets in an idle loop. If a frame is received, a callback function is called and the received data is printed on the console output.

Figure 4.13: Receiver software used for the evaluation

Note: The MAC address is censored in figure 4.13, due to privacy reasons.

42

4.3.3 Results and discussion

Similar to the previous measurements described in "Evaluation of the optical path" no data was received at the PC, due to the Auto-Negotiation procedure. In order to transmit data from the optical path to the Ethernet path, the Auto-Negotiation procedure needs to be completed on the optical side. Otherwise, no data can be forwarded to the Ethernet interface. As a result of this, no data is received by the PC.

5 Conclusion

As stated in the introduction, free space optical communication systems gained more interest in the aerospace industry in the recent years. However, different atmospheric effects need to be considered, such as atmospheric turbulences or fog events, which result in a high attenuation. Radio frequency communication systems, on the other hand, are very robust against turbulences or fog events, which makes them very suitable to achieve a certain quality of service during fog events. Hence, optical communication systems can act as an extension to radio frequency communication systems. However, due to the very high data rates (up to 10 Gbps), optical communication systems outperform radio frequency communication systems. Especially in deep space communication, optical communication gained interest, due to the lack of atmospheric effects in space.

As the measurements show, the Auto-Negotiation procedure needs to be supported by the satellite in order to establish a communication link, due to the Ethernet IEEE 802.3 standard. Otherwise no data can be exchanged between the satellite or the ground station. Since SFP modules are protocol transparent, they can be used as a receiver in combination with i.e. a SFP breakout board, in theory. However, the signal power received at the ground station can be very low depending on the satellite link budget. Therefore, a bigger optical active receiver area is necessary in order to capture enough photons for receiving the satellite signal. Hence, a photo detector with a bigger optical active receiver area needs to be used compared to the photo detector of the SFP module. Another solution would be to pre-amplify the received optical signal using i.e. an erbium doped fibre amplifier.

Future work

Since media converters are not protocol transparent, the optical data needs to be processed in a different way. One solution for translating optical signals into Ethernet frames might be the usage of a SFP breakout board in combination with a SMA PCI card for PCs (see figure 5.1). The SFP module in combination with the SFP breakout board translates the optical signal into an electrical signal. This electrical signal can then be fed into the PCI card. Now the electrical signals are digitized and understandable for the PC. The received data can then be put into Ethernet frames and distributed further into the local are network.

Figure 5.1: Alternative approach optical signal translation

The usage of digitizer PCI cards leads to a much more flexible system design. Satellites can adjust their data rates depending on the bit error rates of the communications link. Due to certain weather conditions (i.e. clouds), the bit error rates might increase. Reducing the data rates, can also reduce the bit error rate, due to the increased bit length during transmission. Hence, more photons are received at the ground station. A system using digitizer PCI cards can cope with changes in the data rate.
Another aspect of using a PCI card is the flexibility in modulation schemes. PPM can also be implemented cost effectively on the receiver software side. Also synchronization with the satellite signal can be problematic, if the data rate is variable or unknown. Preambles in the data stream mitigate this issue and can also be implemented on software side in the system.
The development effort using PCI cards, is mainly on software side. Hence further changes in the system (i.e. PPM implementation, filters, etc.) can be easily implemented and are therefore cost effective for future developments.

Bibliography

[1] D. M. Cornwell, "Nasa's optical communications program for 2017 and beyond," in *2017 IEEE International Conference on Space Optical Systems and Applications (ICSOS)*, 2017, pp. 10–14 (cit. on p. 1).

[2] D. Boroson, B. Robinson, D. Burianek, D. Murphy, and A. Biswas, "Overview and status of the lunar laser communications demonstration," *Proceedings of SPIE - The International Society for Optical Engineering*, vol. 8246, pp. 7–, Feb. 2012. DOI: `10.1117/12.914801` (cit. on p. 1).

[3] DLR, *DLR and ADVA set a new world record in optical free-space data transmission*, [online], Available: `https://www.dlr.de/content/en/articles/news/2018/2/20180510_dlr-and-adva-set-a-new-world-record-in-optical-free-space-data-transmission_27323.html`, [Accessed May 20, 2020] (cit. on p. 1).

[4] A. Biswas, M. Srinivasan, R. Rogalin, S. Piazzolla, J. Liu, B. Schratz, A. Wong, E. Alerstam, M. Wright, W. T. Roberts, J. Kovalik, G. Ortiz, A. Na-Nakornpanom, M. Shaw, C. Okino, K. Andrews, M. Peng, D. Orozco, and W. Klipstein, "Status of nasa's deep space optical communication technology demonstration," in *2017 IEEE International Conference on Space Optical Systems and Applications (ICSOS)*, 2017, pp. 23–27 (cit. on p. 1).

[5] P. Lord, S. Tilley, D. Y. Oh, D. Goebel, C. Polanskey, S. Snyder, G. Carr, S. M. Collins, G. Lantoine, D. Landau, and L. Elkins-Tanton, "Psyche: Journey to a metal world," in *2017 IEEE Aerospace Conference*, 2017, pp. 1–11 (cit. on p. 1).

[6] T. Tolker-Nielsen and G. Oppenhauser, "In-orbit test result of an operational optical intersatellite link between ARTEMIS and SPOT4, SILEX," in *Free-Space Laser Communication Technologies XIV*, G. S. Mecherle, Ed., International Society for Optics and Photonics, vol. 4635,

SPIE, 2002, pp. 1–15. DOI: 10.1117/12.464105. [Online]. Available: https://doi.org/10.1117/12.464105 (cit. on p. 1).

[7] D. Giggenbach, H. Henniger, J. Horwath, N. Perlot, U. Birnbacher, C. Chlestil, M. Gebhart, E. Leitgeb, S. Muhammad, S. Betti, V. Carrozzo, E. Duca, and A. Zamarreno, "Clear sky optics," in *Influence of the Variability of the Propagation Channel on Mobile, Fixed Multimedia and Optical Satellite Communications*. Jan. 2008, ISBN: 978-3-8322-6904-3 (cit. on p. 1).

[8] J. Charles, D. Hoppe, and A. Sehic, "Hybrid rf / optical communication terminal with spherical primary optics for optical reception," May 2011, pp. 171–179, ISBN: 978-1-4244-9686-0. DOI: 10.1109/ICSOS.2011.5783663 (cit. on p. 2).

[9] E. Leitgeb, J. Bregenzer, M. Gebhart, P. Fasser, and A. Merdonig, "Free space optics - broadband wireless supplement to fiber-networks," Jul. 2003, pp. 57–68, ISBN: 0-8194-4775-7. DOI: 10.1117/12.483832 (cit. on p. 4).

[10] J. Hecht, *Understanding Fiber Optics*. May 2015, ISBN: 978-1511445658 (cit. on pp. 6, 7).

[11] I. Kim, B. Mcarthur, and E. Korevaar, "Comparison of laser beam propagation at 785 nm and 1550 nm in fog and haze for optical wireless communications," *Proc. SPIE*, vol. 4214, Feb. 2001. DOI: 10.1117/12.417512 (cit. on pp. 5, 9).

[12] P. Arora and N. Garg, "Simulative analysis of nrz-ook point-to-point free space optical link under continental fog in view of retinal safety," in *2017 International Conference on Computing, Communication and Automation (ICCCA)*, 2017, pp. 619–624 (cit. on p. 5).

[13] A. Majumdar and J. Ricklin, *Free-Space Laser Communications*. Jan. 2008, ISBN: 978-0-387-28652-5. DOI: 10.1007/978-0-387-28677-8 (cit. on p. 7).

[14] E. Leitgeb, M. Gebhart, P. Fasser, J. Bregenzer, and J. Tanczos, "Impact of atmospheric effects in free space optics transmission systems," *Proc SPIE*, Apr. 2003. DOI: 10.1117/12.483802 (cit. on pp. 8, 9).

[15]   G. Soni, "Experimental evaluation determination of free space optical link performance at 532nm wavelength under rain attenuation conditions its comparison with 850nm wavelength," in *2017 International Conference on Big Data Analytics and Computational Intelligence (ICBDAC)*, 2017, pp. 447–450 (cit. on p. 9).

[16]   A. Z. Suriza, A. K. Wajdi, M. I. Rafiqul, and A. W. Naji, "Preliminary analysis on the effect of rain attenuation on free space optics (fso) propagation measured in tropical weather condition," in *Proceeding of the 2011 IEEE International Conference on Space Science and Communication (IconSpace)*, 2011, pp. 96–101 (cit. on p. 9).

[17]   K. Rammprasath and S. Prince, "Analyzing the cloud attenuation on the performance of free space optical communication," in *2013 International Conference on Communication and Signal Processing*, 2013, pp. 791–794 (cit. on pp. 10, 11).

[18]   H. Kaushal, V. Kumar, A. Dutta, H. Aennam, V. K. Jain, S. Kar, and J. Joseph, "Experimental study on beam wander under varying atmospheric turbulence conditions," *IEEE Photonics Technology Letters*, vol. 23, no. 22, pp. 1691–1693, 2011 (cit. on p. 10).

[19]   M. Uysal, C. Capsoni, A. Boucouvalas, and E. Udvary, *Optical Wireless Communications – An Emerging Technology*. Jan. 2017, ISBN: 978-3-319-30200-3. DOI: 10.1007/978-3-319-30201-0 (cit. on pp. 10, 12).

[20]   C. Lamprecht, P. Bekhrad, H. Ivanov, and E. Leitgeb, "Modelling the refractive index structure parameter: A ResNet approach," in *2020 International Conference on Broadband Communications for Next Generation Networks and Multimedia Applications (CoBCom) (CoBCom 2020)*, Graz, Austria, Jul. 2020 (cit. on pp. 12, 13).

[21]   Z. Ghassemlooy, J. Perez, and E. Leitgeb, "On the performance of fso communications links under sandstorm conditions," in *Proceedings of the 12th International Conference on Telecommunications*, 2013, pp. 53–58 (cit. on p. 14).

[22]   M. Belkheir and M. Rouissat, "Performance analysis of rz-ppm coding in optical wireless systems," in *2019 6th International Conference on Image and Signal Processing and their Applications (ISPA)*, 2019, pp. 1–3 (cit. on p. 19).

[23] Hyuncheol Park and J. R. Barry, "Modulation analysis for wireless infrared communications," in *Proceedings IEEE International Conference on Communications ICC '95*, vol. 2, 1995, 1182–1186 vol.2 (cit. on p. 21).

[24] M. Rouissat, R. Borsali, and M. Chick-Bled, "Dual amplitude-width digital pulse interval modulation for optical wireless communications," *International Journal of Computer Science Issues*, vol. Vol. 9, pp. 187–191, May 2012 (cit. on p. 21).

[25] T. Y. Elganimi, "Studying the ber performance, power- and bandwidth-efficiency for fso communication systems under various modulation schemes," in *2013 IEEE Jordan Conference on Applied Electrical Engineering and Computing Technologies (AEECT)*, 2013, pp. 1–6 (cit. on p. 21).

[26] "IEEE standard for ethernet," *IEEE Std 802.3-2018 (Revision of IEEE Std 802.3-2015)*, pp. 1–5600, 2018 (cit. on p. 41).

Appendix A - Bit rate measurement results

Index	Direct Ethernet Link	Optical Ethernet Transceiver Modem
1	4.11E+08	4.31E+08
2	4.41E+08	4.58E+08
3	5.15E+08	5.01E+08
4	5.19E+08	5.28E+08
5	5.35E+08	5.21E+08
6	5.28E+08	5.02E+08
7	4.24E+08	4.22E+08
8	5.03E+08	5.00E+08
9	5.17E+08	5.05E+08
10	4.89E+08	5.18E+08
11	5.28E+08	5.14E+08
12	4.64E+08	4.26E+08
13	4.37E+08	4.61E+08
14	5.27E+08	5.20E+08
15	5.22E+08	5.15E+08
16	5.36E+08	5.04E+08
17	5.30E+08	4.18E+08
18	4.30E+08	4.86E+08
19	4.56E+08	5.01E+08
20	5.26E+08	5.05E+08
21	5.25E+08	4.23E+08
22	5.33E+08	4.31E+08
23	4.31E+08	5.14E+08
24	4.98E+08	5.14E+08
25	5.21E+08	5.22E+08
26	5.22E+08	4.86E+08
27	4.88E+08	4.30E+08
28	4.28E+08	5.13E+08
29	4.94E+08	5.32E+08
30	5.09E+08	5.18E+08
31	4.25E+08	5.16E+08
32	5.19E+08	4.23E+08
33	5.33E+08	5.14E+08
34	5.12E+08	5.03E+08

Index	Direct Ethernet Link	Optical Ethernet Transceiver Modem
35	4.28E+08	5.20E+08
36	5.29E+08	5.38E+08
37	5.22E+08	4.23E+08
38	4.24E+08	5.10E+08
39	4.77E+08	5.07E+08
40	5.13E+08	5.01E+08
41	5.12E+08	5.03E+08
42	4.28E+08	4.30E+08
43	5.36E+08	4.93E+08
44	5.34E+08	5.26E+08
45	5.28E+08	5.32E+08
46	4.22E+08	4.96E+08
47	5.02E+08	4.31E+08
48	5.26E+08	5.29E+08
49	5.13E+08	5.30E+08
50	5.24E+08	5.08E+08
51	5.35E+08	4.20E+08
52	5.24E+08	5.00E+08
53	5.18E+08	5.02E+08
54	5.05E+08	4.21E+08
55	5.26E+08	4.93E+08
56	5.13E+08	5.07E+08
57	5.15E+08	5.00E+08
58	4.97E+08	5.12E+08
59	4.33E+08	4.21E+08
60	5.17E+08	5.22E+08
61	5.00E+08	5.22E+08
62	5.18E+08	5.16E+08
63	5.07E+08	4.99E+08
64	4.21E+08	4.27E+08
65	5.21E+08	5.09E+08
66	5.26E+08	5.19E+08
67	5.11E+08	5.13E+08
68	4.29E+08	4.18E+08

Index	Direct Ethernet Link	Optical Ethernet Transceiver Modem
69	4.84E+08	5.06E+08
70	4.22E+08	5.23E+08
71	5.10E+08	4.99E+08
72	5.10E+08	5.17E+08
73	5.15E+08	4.21E+08
74	5.10E+08	4.99E+08
75	4.22E+08	5.27E+08
76	5.12E+08	5.25E+08
77	5.11E+08	5.27E+08
78	5.17E+08	4.24E+08
79	4.31E+08	4.92E+08
80	5.16E+08	5.29E+08
81	5.17E+08	5.14E+08
82	5.24E+08	5.07E+08
83	5.00E+08	4.46E+08
84	4.22E+08	4.26E+08
85	5.26E+08	4.82E+08
86	5.14E+08	5.02E+08
87	5.16E+08	5.00E+08
88	4.72E+08	5.07E+08
89	4.24E+08	4.21E+08
90	5.25E+08	5.14E+08
91	5.03E+08	5.12E+08
92	5.31E+08	5.14E+08
93	4.33E+08	4.60E+08
94	4.99E+08	4.24E+08
95	5.24E+08	5.11E+08
96	5.24E+08	5.16E+08
97	5.05E+08	5.14E+08
98	4.28E+08	4.96E+08
99	5.25E+08	4.16E+08
100	5.32E+08	4.70E+08

Appendix B - 1000BASE-BX SFP1490nmTX/1550nmRX

FS

1000BASE-BX SFP 1490nmTX/1550nmRX 80km DOM Transceiver

SFP-GE-BX80

Application

- Switch to Switch Interface
- Fast Ethernet
- Switched Backplane Applications
- Router/Server Interface
- Other Optical Links

Features

- Operating data rate Up to 1.25Gb/s
- Two types:
   A:1490nm DFB transmitter /1550nm receiver
   B:1550nm DFB transmitter/1490nm receiver
- Up to 80km on 9/125μm SMF
- Hot-pluggable SFP footprint
- BIDI LC/UPC type pluggable optical
   interface

- Low power dissipation
- Metal enclosure, for lower EMI
- RoHS compliant and lead-free
- Support Digital Diagnostic Monitor
   interface
- Single +3.3V power supply

- Case operating temperature:
   Commercial: 0°C ~ 70°C
   Extended: -20°C ~ 85°C
   Industrial: -40°C ~ 85°C
- Compliant with MSA SFP Specification
- Compliant with SFF-8472
- Compliant with IEEE 802.3z

Appendix B - 1000BASE-BX SFP1490nmTX/1550nmRX

FS

Description

FS.COM SFP-GE-BX80 SFP transceiver is compatible with the Small Form Factor Pluggable Multi-Sourcing Agreement (MSA). The transceiver consists of five sections: the LD driver, the limiting amplifier, the digital diagnostic monitor, the 1490nm FP laser (the 1550nm DFB laser)and the PIN/TIA. The module data link up to 80km in 9/125um Single-mode fiber.

This transceiver meets the Small Form Pluggable (SFP) industry standard package utilizing an integral LC-Bi-dirictional optical interface connector. An enhanced Digital Diagnostic Monitoring Interface compliant with SFF-8472 has been incorporated into the transceiver. It allows real time access to the transceiver operating parameters such as transceiver temperature, laser bias current, transmitted optical power, received optical power and transceiver supply voltage by reading a built-in memory with I²C interface.

The optical output can be disabled by a LVTTL logic high-level input of Tx Disable, and the system also can disable the module via I²C. Tx Fault is provided to indicate that degradation of the laser. Loss of signal (LOS) output is provided to indicate the loss of an input optical signal of receiver or the link status with partner. The system can also get the LOS (or Link)/Disable/Fault information via I²C register access.

Product Specifications

I.General Specifications

Parameter	Symbol	Min	Typ.	Max	Unit
Bit Rate	BR			1.25	Gb/sec
Max.Supported Link Length	Lmax			80	km

Appendix B - 1000BASE-BX SFP1490nmTX/1550nmRX

≋FS

II. Absolute Maximum Ratings

Parameter	Symbol	Min	Typ.	Max	Unit	Ref.
Storage Temperature	T_S	-40		85	ºC	
Storage Ambient Humidity	H_A	5		95	%	
Power Supply Voltage	V_{CC}	-0.5		4	V	
Signal Input Voltage		-0.3		Vcc+0.3	V	
Receiver Damage Threshold		+3			dBm	
Lead Soldering Temperature/Time	T_{sold}			260/10	ºC/sec	Note 1
Lead Soldering Temperature/Time	T_{sold}			360/10	ºC/sec	Note 2

Notes:

1. Suitable for wave soldering.

2. Only for soldering by iron.

III. Electrical Characteristics

Parameter	Symbol	Min	Typ.	Max	Unit	Ref.
		0		70		SFP-GE-BX80-C
Case Operating Temperature	T_{case}	-20		85	ºC	SFP-GE-BX80-E
		-40		85		SFP-GE-BX80-I

Appendix B - 1000BASE-BX SFP1490nmTX/1550nmRX

FS

Parameter	Symbol	Min	Typ.	Max	Unit	Ref.
Ambient Humidity	H_A	5		70	%	Non-condensing
Power Supply Voltage	V_{CC}	3.13	3.3	3.47	V	
Power Supply Current	I_{CC}			280	mA	
Data Rate			1250/1250		Mbps	TX Rate/RX Rate
Transmission Distance				80	km	
Coupled Fiber			Single mode fiber			9/125µm G.652

Transmitter

Parameter	Symbol	Min	Typ.	Max	Unit	Ref.
Total Supply Current	I_{CC}			A	mA	
Transmitter Disable Input-High	V_{DISH}	2		Vcc+0.3	V	Note 1
Transmitter Disable Input-Low	V_{DISL}	0		0.8	V	LVTTL
Fault Input-High	V_{TxFH}	Transmitter2		Vcc+0.3	V	LVTTL
Transmitter Fault Input-Low	V_{TxFL}	0		0.8	V	LVTTL

Receiver

Parameter	Symbol	Min	Typ.	Max	Unit	Ref.
Total Supply Current	I_{CC}			B	mA	Note 1
LOS Output Voltage-High	V_{LOSH}	2		V_{CC}+0.3	V	LVTTL
LOS Output Voltage-Low	V_{LOSL}	0		0.8	V	LVTTL

Note:

1. A (TX) + B (RX) = 280mA   (Not include termination circuit)

Appendix B - 1000BASE-BX SFP1490nmTX/1550nmRX

FS

IV. Optical Characteristics

Parameter	Symbol	Min	Typ.	Max	Unit	Ref.
Transmitter						
Average Output Power	P_{OUT}	-2		+3	dBm	
		-5		0		
Extinction Ratio	ER	9			dB	
Center Wavelength	λ_c	1470	1490	1510	nm	MQEL-K80B45
		1530	1550	1570		MQEL-K80B54
Spectrum Width (RMS)	σ			1	nm	FP Laser(TX:1490nm)
Side Mode Suppression Ratio	SMSR	30			dB	DFB Laser(TX:1550nm)
Spectrum Bandwidth(-20dB)	σ			1	nm	
Transmitter OFF Output Power	P_{OFF}			-45	dBm	
Jitter p-p	t_J			0.1	UI	Note 1
Output Eye Mask	Compliant with IEEE802.3 z (class 1 laser safety)					Note 2
Receiver						
Input Optical Wavelength	λ_{IN}	1530	1550	1570	nm	MQEL-K80B45
		1470	1490	1510		MQEL-K80B54

FS

Receiver Sensitivity	P_{IN}			-24	dBm	Note 3
InputSaturation Power (Overload)	P_{SAT}	-3			dBm	
Loss of Signal Assert	P_A	-45			dBm	
Loss of Signal De-assert	P_D			-23.5	dBm	Note 4
LOS Hysteresis	P_D-P_A	0.5		6	dB	

Notes:

1. Measure at 2^7-1 NRZ PRBS pattern.

2. Transmitter eye mask definition.
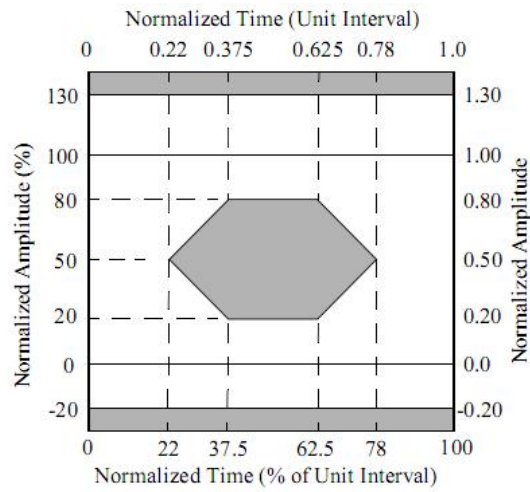
3. Measured with light source 1490nm(1310nm), ER=9dB; BER =<10^-12 @PRBS=2^7-1 NRZ

4. When LOS De-asserted, the RX data+/- output is signal output.

Appendix C - 1000BASE-BX SFP1550nmTX/1490nmRX

FS

1000BASE-BX SFP 1550nmTX/1490nmRX 80km DOM Transceiver

SFP-GE-BX80

Application

- Switch to Switch Interface
- Fast Ethernet
- Switched Backplane Applications
- Router/Server Interface
- Other Optical Links

Features

- Operating data rate Up to 1.25Gb/s
- Two types:
  A:1490nm DFB transmitter /1550nm receiver
  B:1550nm DFB transmitter/1490nm receiver
- Up to 80km on 9/125μm SMF
- Hot-pluggable SFP footprint
- BIDI LC/UPC type pluggable optical interface

- Low power dissipation
- Metal enclosure, for lower EMI
- RoHS compliant and lead-free
- Support Digital Diagnostic Monitor interface
- Single +3.3V power supply

- Case operating temperature:
  Commercial: 0°C ~ 70°C
  Extended: -20°C ~ 85°C
  Industrial: -40°C ~ 85°C
- Compliant with MSA SFP Specification
- Compliant with SFF-8472
- Compliant with IEEE 802.3z

Appendix C - 1000BASE-BX SFP1550nmTX/1490nmRX

FS

Description

FS.COM SFP-GE-BX80 SFP transceiver is compatible with the Small Form Factor Pluggable Multi-Sourcing Agreement (MSA). The transceiver consists of five sections: the LD driver, the limiting amplifier, the digital diagnostic monitor, the 1490nm FP laser (the 1550nm DFB laser)and the PIN/TIA. The module data link up to 80km in 9/125um Single-mode fiber.

This transceiver meets the Small Form Pluggable (SFP) industry standard package utilizing an integral LC-Bi-dirictional optical interface connector. An enhanced Digital Diagnostic Monitoring Interface compliant with SFF-8472 has been incorporated into the transceiver. It allows real time access to the transceiver operating parameters such as transceiver temperature, laser bias current, transmitted optical power, received optical power and transceiver supply voltage by reading a built-in memory with I²C interface.

The optical output can be disabled by a LVTTL logic high-level input of Tx Disable, and the system also can disable the module via I²C. Tx Fault is provided to indicate that degradation of the laser. Loss of signal (LOS) output is provided to indicate the loss of an input optical signal of receiver or the link status with partner. The system can also get the LOS (or Link)/Disable/Fault information via I²C register access.

Product Specifications

I.General Specifications

Parameter	Symbol	Min	Typ.	Max	Unit
Bit Rate	BR			1.25	Gb/sec
Max.Supported Link Length	Lmax			80	km

Appendix C - 1000BASE-BX SFP1550nmTX/1490nmRX

FS

II. Absolute Maximum Ratings

Parameter	Symbol	Min	Typ.	Max	Unit	Ref.
Storage Temperature	T_S	-40		85	℃	
Storage Ambient Humidity	H_A	5		95	%	
Power Supply Voltage	V_{CC}	-0.5		4	V	
Signal Input Voltage		-0.3		Vcc+0.3	V	
Receiver Damage Threshold		+3			dBm	
Lead Soldering Temperature/Time	T_{sold}			260/10	℃/sec	Note 1
Lead Soldering Temperature/Time	T_{sold}			360/10	℃/sec	Note 2

Notes:

1. Suitable for wave soldering.

2. Only for soldering by iron.

III. Electrical Characteristics

Parameter	Symbol	Min	Typ.	Max	Unit	Ref.
Case Operating Temperature	T_{case}	0		70	℃	SFP-GE-BX80-C
		-20		85		SFP-GE-BX80-E
		-40		85		SFP-GE-BX80-I

Appendix C - 1000BASE-BX SFP1550nmTX/1490nmRX

FS

Parameter	Symbol	Min	Typ.	Max	Unit	Ref.
Ambient Humidity	H_A	5		70	%	Non-condensing
Power Supply Voltage	V_{CC}	3.13	3.3	3.47	V	
Power Supply Current	I_{CC}			280	mA	
Data Rate			1250/1250		Mbps	TX Rate/RX Rate
Transmission Distance				80	km	
Coupled Fiber			Single mode fiber			9/125μm G.652
Transmitter						
Total Supply Current	I_{CC}			A	mA	
Transmitter Disable Input-High	V_{DISH}	2		Vcc+0.3	V	Note 1
Transmitter Disable Input-Low	V_{DISL}	0		0.8	V	LVTTL
Transmitter Fault Input-High	V_{TxFH}	2		Vcc+0.3	V	LVTTL
Transmitter Fault Input-Low	V_{TxFL}	0		0.8	V	LVTTL
Receiver						
Total Supply Current	I_{CC}			B	mA	Note 1
LOS Output Voltage-High	V_{LOSH}	2		V_{CC}+0.3	V	LVTTL
LOS Output Voltage-Low	V_{LOSL}	0		0.8	V	LVTTL

Note:

1. A (TX) + B (RX) = 280mA   (Not include termination circuit)

Appendix C - 1000BASE-BX SFP1550nmTX/1490nmRX

FS

IV. Optical Characteristics

Parameter	Symbol	Min	Typ.	Max	Unit	Ref.
Transmitter						
Average Output Power	P_{OUT}	-2		+3	dBm	
		-5		0		
Extinction Ratio	ER	9			dB	
Center Wavelength	λ_c	1470	1490	1510	nm	MQEL-K80B45
		1530	1550	1570		MQEL-K80B54
Spectrum Width (RMS)	σ			1	nm	FP Laser(TX:1490nm)
Side Mode Suppression Ratio	SMSR	30			dB	DFB Laser(TX:1550nm)
Spectrum Bandwidth(-20dB)	σ			1	nm	
Transmitter OFF Output Power	P_{OFF}			-45	dBm	
Jitter p-p	t_J			0.1	UI	Note 1
Output Eye Mask	Compliant with IEEE802.3 z (class 1 laser safety)					Note 2
Receiver						
Input Optical Wavelength	λ_{IN}	1530	1550	1570	nm	MQEL-K80B45
		1470	1490	1510		MQEL-K80B54

Appendix C - 1000BASE-BX SFP1550nmTX/1490nmRX

FS

Receiver Sensitivity	P_{IN}			-24	dBm	Note 3
InputSaturation Power (Overload)	P_{SAT}	-3			dBm	
Loss of Signal Assert	P_A	-45			dBm	
Loss of Signal De-assert	P_D			-24.5	dBm	Note 4
LOS Hysteresis	P_D-P_A	0.5		6	dB	

Notes:

1. Measure at 2^7-1 NRZ PRBS pattern.

2. Transmitter eye mask definition.
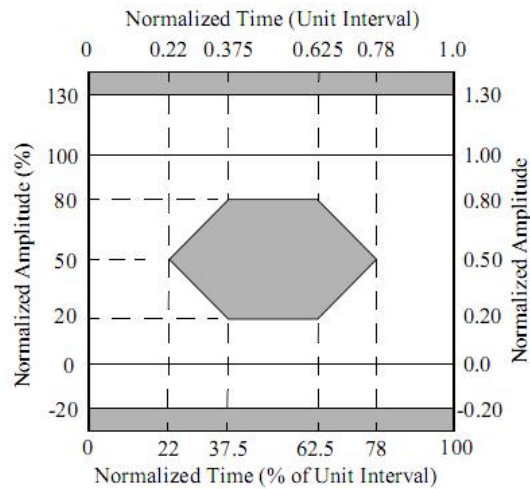
3. Measured with light source 1490nm(1310nm), ER=9dB; BER =<10^-12 @PRBS=2^7-1 NRZ

4. When LOS De-asserted, the RX data+/- output is signal output.

Appendix D - Ethernet Media Converter

NETWORKS

ETHERNET MEDIA CONVERTER USER MANUAL

FS

1. Overview

Since all the FS Media Converter models represented in this manual do not share all the same features, refer to the product or its corresponding parameters to determine which of the following sections or items within the sections apply to the enclosed product. For example, not all of the LEDs defined in the status reference chart may be featured on your media converter.

2. Package contents

The following items should be found in your package:
• 1x The Media Converter
• 1x AC-DC Power Adapter (for external models) or Power Cord (for internal models)
• 1x The User's Manual

NOTE: Make sure that the package contains the above items. If any of the listed items are damaged or missing, please notify your Account Manager immediately.

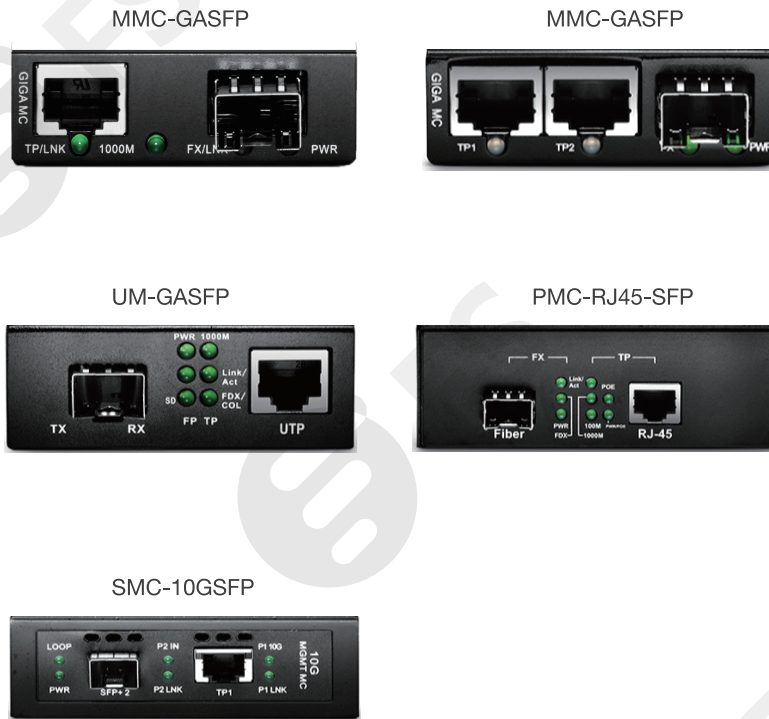# Chapter 1 Product Appearance

1.1 Port Locations and Layouts

MMC-GASFP

MMC-GASFP

UM-GASFP

PMC-RJ45-SFP

SMC-10GSFP

Figure 1-1

71

1.2 LED Indicators

Front panel LEDs provide at-a-glance network status and real-time connectivity information. Each of them has its own specific meaning as shown in the table below. Not all models will have all of the LED Indicators described.

LED		Status	Indication
PWR		ON	Power is on.
		OFF	Power is off.
FX/FP	LNK/ACT	ON	Fiber port is linked.
		Blinking	Fiber port is actively transmitting data.
		OFF	Fiber link is fail.
TP	LNK/ACT	ON	Copper port is linked.
		Blinking	Copper port is actively transmitting data.
		OFF	Copper link is fail.
1000M		ON	1000M (TP).
		OFF	100M/10M (TP).
SD		ON	Fiber port singal is detected.
		OFF	Fiber port singal does not detected.
FDX/COL		ON	Full duplex.
		OFF	Half duplex.
LOOP		ON	Loopback is on.
		OFF	Loopback is off.

Table 1-1

72

1.3 DIP Switch Setting

1.3.1 Mini Media Converter DIP Switches (MMC-GASFP)

1 RJ45 to 1 SFP

NO	Function		Status	Description
1	LFP Function		OFF	Disable.
			ON	Enable.
2	Forward Mode*	H Bit	OFF/OFF	Store and forward.
			OFF/ON	Modified cut through.
3		L Bit	ON/OFF	Smart pass through.
			ON/ON	Pass through.
4	FX 100M		OFF	FX 1000M.
			ON	FX 100M.

* Combined keys

Table 1-2

NO	Function	Status	Description
1	Reserved	X	X.
		OFF	Normal.
2	Jumbo Frame	ON	Up to 9KB.
		OFF/ON	Modified cut through.
3	Port Isolation*	OFF	Disable.
		ON	Enable.
4	FX 100M	OFF	FX 1000M.
		ON	FX 100M.

* Between two RJ-45 ports

Table 1-3

73

1.3.2 PoE Media Converter DIP Switches (PMC-RJ45-SFP)

NO	Function	Status	Description
SW1-1	ENROM*	OFF	Disable.
		ON	Enable EEPROM SET.
SW1-2	FX100M*	OFF	FX 1000M(default).
		ON	FX 100M.
SW1-3	NULL	OFF	Reserved.
		ON	
SW1-4	LFP*	OFF	Disable.
		ON	Enable.
SW1-5	MODE1**	OFF/OFF	Store and Forward mode.
		OFF/ON	Modified cut through mode.
SW1-6	MODE0**	ON/OFF	Smart pass through mode.
		ON/ON	Pass through mode.

*,** combined keys.

The function of SW2 or SW4 can be effective when SW1 is on.

Table 1-4

Chapter 2 Installation

2.1 Stand-alone Installation

To install the media converter stand-alone, on a desktop or shelf, simply follow the steps below:

Step 1: Place the media converter on a flat, secure surface (such as a desk) leaving ample space around the unit for ventilation.

Step 2: Connect the Cat5e (or better) Ethernet cable to the RJ45 port of the media converter (This port is auto-negotiating). And connect the other end of the Cat5e (or better) Ethernet cable into your network device (switch, PC, router, etc.)

Step 3: Insert a SFP module into the open SFP slot, connect the fiber optic cable to the SFP transceiver. Both multimode cabling and single mode cabling are supported. Make sure both side of the SFP transfer are with the same media type. Plug the other end of the fiber optic cable to the fiber network.

Step 4: Connect the power adapter to the media converter, and plug the another end to the AC socket. The corresponding LED is ON for correct connection.

1000Base-SX/LX
SFP transceiver

10/100/1000Base-T UTP

1000Base-SX/LX
LC Fiber

Figure 2-1
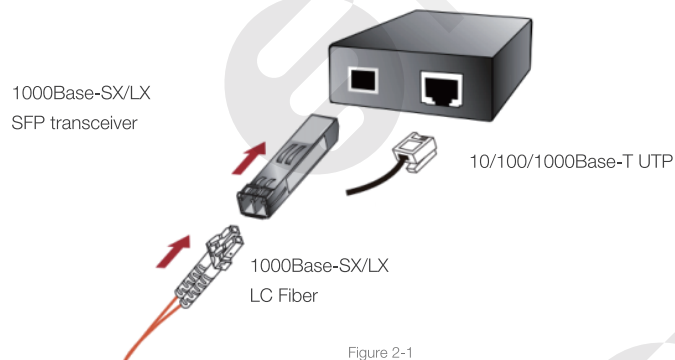
Chapter 3 Technical Specifications

Models	UM-GASFP	MMC-GASFP	MMC-GASFP	PMC-RJ45-SFP	SMC-10GSFP	MFMC-12DP
Standards	IEEE802.3U, IEEE802.3Z, 1000Base-TX				IEEE802.3an, IEEE802.3ae	N/A
Ports	1× RJ45 to 1× SFP	1× RJ45 to 1× SFP	2× RJ45 to 1× SFP	1× RJ45 to 1× SFP	1× RJ45 to 1× SFP+	12 Slots
Compatible Fiber Types	Depends on the transceiver modules					N/A
Optical wavelength	Depends on the transceiver modules					N/A
Duplex Modes	Full/Half					N/A
Auto MDIX	Yes					N/A
Power Supply	AC 100-240V 50/60Hz					
Operating Temperature	0°C to 50°C	0°C to 40°C	0°C to 40°C	0°C to 50°C		
Storage Temperature	-20°C to 85°C				-10°C to 70°C	-20°C to 70°C
Humidity	90% max, non-condensing					
Dimension (WxDxH)	70 x 95 x 26 (mm)	60 x 90 x 20 (mm)		110 x 140 x 40 (mm)	173 × 106 × 33 (mm)	485 x 270 x 44.5 (mm)

Table 3-1

76

Appendix E - Fiber optic coupler

THOR LABS

Boxed Wideband Fiber Optic Coupler
1550 nm, 50:50 Ratio

BXC15

Description

Thorlabs' BXC15 single mode wideband fiber optic boxed coupler is designed to operate from 1450 to 1650 nm with ≤0.15 dB of excess loss. The ruggedized and compact housing provides durability and space efficiency for laboratory setups or experimental arrangements. It is offered with FC/APC bulkheads for both the input and output ports.

Specifications

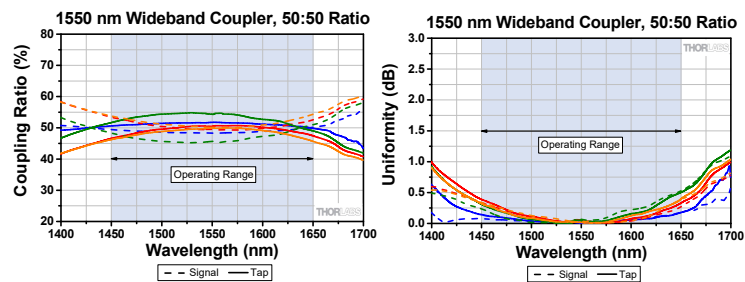| BXC15	
Coupling Ratio[a]	50:50
Coupling Ratio Tolerance	±5.0%
Center Wavelength	1550 nm
Minimum Bandwidth	±100 nm
Insertion Loss[a]	≤3.6 dB / ≤3.6 dB
Excess Loss[a]	≤0.15 dB (Typical)
Uniformity[a]	≤0.5 dB
Polarization-Dependent Loss (PDL)[a]	≤0.15 dB
Optical Return Loss (ORL) / Directivity[a]	≥60 dB
Max Power Level[b]	1 W
Fiber Type[c]	SMF-28
Fiber Cut-Off Wavelength	≤1260 nm
Fiber NA	0.14
Optical Ports	2.0 mm Narrow-Key FC/APC Bulkheads
Port Configuration	2x2
Dimensions	1.13" x 2.38" x 3.55" (28.7 mm x 60.4 mm x 90.1 mm)
Operating Temperature Range	-40 to 85 °C
Storage Temperature Range	-40 to 85 °C

a.   All values are specified at room temperature over the bandwidth and measured through IN 1 without connectors or bulkheads.
b.   Specifies the total maximum power allowed through the component. Coupler performance and reliability under high-power conditions must be determined within the user's setup. See Usage Tips for safety and handling information.
c.   Corning SMF-28 fiber type will be specified on the documentation that ships with the coupler.

Specifications Subject
to Change without Notice

Typical Performance Plots

1550 nm Wideband Coupler, 50:50 Ratio
(Coupling Ratio (%) vs Wavelength (nm))

1550 nm Wideband Coupler, 50:50 Ratio
(Uniformity (dB) vs Wavelength (nm))

These persistence plots show the coupling ratio and uniformity performance of four BXC15 couplers (tap and signal outputs from the same coupler are indicated by matching colors on each graph). The blue-shaded region denotes the coupler's full operating wavelength range. All data was measured without connectors.

Usage Tips

1) Before connecting a component to a system, make sure the light source is turned off. Inspect both the input and output fiber ends; debris or contamination on the end face can lead to fiber damage when operated at high powers. Fiber bulkhead cleaners are available on the Thorlabs website.

2) After connecting the component, the system should be tested and aligned using a light source at low power. The system power can be ramped up slowly to the desired output power while periodically verifying all components are properly aligned and that coupling efficiency is not changing with respect to optical launch power.

October 3, 2019
TTN187518-S01, Rev C
www.thorlabs.com/contact

www.thorlabs.com